RIGA TECHNICAL UNIVERSITY

Pauls Pāvils Ārgalis

RECYCLING OF WOOD-CEMENT MANUFACTURING WASTE INTO INNOVATIVE BUILDING MATERIALS

Summary of the Doctoral Thesis

RTU Press
Riga 2025

RIGA TECHNICAL UNIVERSITY
Faculty of Civil and Mechanical Engineering
Institute of Sustainable Building Materials and Engineering Systems

Pauls Pāvils Ārgalis
Doctoral Student of the Study Programme "Civil Engineering"

RECYCLING OF WOOD-CEMENT MANUFACTURING WASTE INTO INNOVATIVE BUILDING MATERIALS

Summary of the Doctoral Thesis

Scientific supervisors:
Professor Dr. sc. ing.
DIĀNA BAJĀRE
Senior Researcher Dr. sc. ing.
MĀRIS ŠINKA

RTU Press
Riga 2025

Ārgalis, P. P. Recycling of Wood-Cement Manufacturing Waste into Innovative Building Materials. Summary of the Doctoral Thesis. Riga: RTU Press, 2025. 50 p.

Published in accordance with the decision of the Promotion Council "RTU P-06" of June 4, 2025, Minutes No. 04030- 9.6/6.

The Thesis was developed at the Institute of Sustainable Building Materials and Engineering Systems of the Faculty of Civil and Mechanical Engineering, Riga Technical University. The Thesis includes studies on the European Green Deal, the sustainability of the Latvian construction sector, the development of a suitable cementitious binder from industrial waste, its properties, its potential application in the production of biocomposites, and the life cycle assessment of the produced biocomposites.

Firstly, I would like to thank Cewood Ltd. for showing me how their products are manufactured and supplying the waste materials for me to experiment with; special thanks to Jānis, Rūdolfs, Kristaps, and Ingars for answering all my questions.

Secondly, I would like to thank PhD Laura Vitola for the tremendous help given me. Starting with a change in thinking about civil engineering as a science (my previous major was materials science), consulting about experiments in the laboratory, and proofreading some of the sections in the Thesis. I would also like to thank Dr. sc. ing. Ģirts Būmanis for his expertise in the experimental part of the Thesis and Mg. sc. ing. Liga Puzule for calculating the LCA data and proofreading the analysis and discussion of it. I would also like to thank my supervisors for all the hard discussions I have put them through, and all the other colleagues who helped me through this journey.

Thirdly, I am most grateful to my family, who have been close to me, motivating and cheering me on during this process. Thank you, and as once "a great man" said:

"It is not going to be better than it will be!"

Cover picture from CEWOOD Ltd, author – Māris Šmits.

https://doi.org/10.7250/9789934372032
ISBN 978-9934-37-203-2 (pdf)

DOCTORAL THESIS PROPOSED TO RIGA TECHNICAL UNIVERSITY FOR PROMOTION TO THE SCIENTIFIC DEGREE OF DOCTOR OF SCIENCE

To be granted the scientific degree of Doctor of Science (PhD), the present Doctoral Thesis has been submitted for defence at the open meeting of RTU Promotion Council on September 19, 2025, at 14.00 at the Faculty of Civil and Mechanical Engineering of Riga Technical University, 6A Ķīpsalas Street, Room 342.

OFFICIAL REVIEWERS

Associate Professor Dr. sc. ing. Līva Pupure,
Riga Technical University

Professor PhD Jiří Zach,
Brno University of Technology, Czech Republic

Professor PhD Džigita Nagrockienė,
Vilnius Gediminas Technical University, Lithuania

DECLARATION OF ACADEMIC INTEGRITY

I hereby declare that the Doctoral Thesis submitted for review to Riga Technical University for promotion to the scientific degree of Doctor of Science (PhD) is my own. I confirm that this Doctoral Thesis has not been submitted to any other university for promotion to a scientific degree.

Pauls Pāvils Ārgalis ……. (signature)
Date: ……

The Doctoral Thesis has been written in English. It consists of an Introduction, eight chapters, Conclusions, 99 figures, and 28 tables; the total number of pages is 139. The Bibliography contains 245 titles.

TABLE OF CONTENTS

ABBREVIATIONS USED IN THE THESIS 6

GENERAL DESCRIPTION OF THE THESIS 7

Research topicality and problem statement 7
The aim of the Thesis 8
Objectives of the Thesis 8
The scientific novelty of the research 8
Practical relevance of the Thesis 9
Research methodology 10
Limits of research 11
Theses for defence 11
Composition and scope of the Thesis 12
Approbation of the Thesis results 12
List of publications 13

1. ENVIRONMENTAL IMPACT AND CLIMATE STRATEGIES IN LATVIA 14

2. WOOD-WOOL CEMENT PANELS 15

3. REACTIVATION OF PORTLAND CEMENT-BASED BINDERS 16

4. MATERIALS AND METHODS 17

4.1. Raw Materials 17
Sanding Dust (SD) 17
Production Line Waste (PLW) 17
Other Materials 18
4.2. Modification of the Sanding Dust 18
4.3. Characterisation Techniques 18
4.4. Life Cycle Assessment 19

5. MILLING EFFECT ON THE REACTIVATION OF THE SANDING DUST 20

5.1. Sanding Dust Reactivated by Planetary Ball Mill 20
Mix Design and Sample Preparation 20
Results 20
5.2. Sanding Dust Reactivated by Collision Milling 21
Mix Design and Sample Preparation 21
Results 21
5.3. Sanding Dust Reactivated by Vibration Mill 22
Mix Design and Sample Preparation 22
Results 22
5.4. Chapter Summary 23

6. HEAT TREATMENT EFFECT ON THE REACTIVATION OF THE SANDING DUST 24

6.1. Sanding Dust Reactivated by Heating in Muffle Furnace 24
Mix Design and Sample Preparation 24
Results 24
6.2. Chapter Summary 29

7. CHARACTERISATION AND PERFORMANCE OF BIOCOMPOSITES WITH REACTIVATED BINDERS 30

7.1. Biocomposites with Mechanically Activated Binder 30
Mix Design and Sample Preparation 30
Results and Discussion 30
7.2. Biocomposites with Thermally Treated Sanding Dust 32
7.2.1. Biocomposites with Sanding Dust Treated at 450 ℃ 32
Mix Design and Sample Preparation 32
Results 32
7.2.2. Biocomposites with Sanding Dust Treated at 600 ℃ 34
Mix Design and Sample Preparation 34
Results 35
7.3. Biocomposites with CEM II/A-LL 42.5 N 37
Mix Design and Sample Preparation 37
Results and Discussion 38
7.4. Demonstration of Biocomposites 39
7.5. Chapter Summary 41

8. LIFE CYCLE ASSESSMENT OF THE DEVELOPED BUILDING MATERIALS 42

CONCLUSIONS 43

REFERENCES 44

ABBREVIATIONS USED IN THE THESIS

CDW – Construction and Demolition Waste
LEGMC – Latvian Environment, Geology and Meteorology Centre
EU – European Union
NECP – National Energy and Climate Plan
nZEB – nearly Zero Emission Buildings
GPP – Green Public Procurement
WMP – Waste Management Plan
URC – Urban Recycling Centre
LCA – Life Cycle Assessment
WWCP – Wood-Wool Cement Panels
CEM I – > 95 % cement clinker binder ≥ 52.5 MPa on day 28
CEM II/A-LL 42.5 N – cement clinker and limestone binder ≥ 42.5 MPa on day 28
PLW – Production Line Waste
TG – Thermogravimetry
DTA – Differential Thermal Analysis
XRF – X-Ray Fluorescence
XRD – X-Ray Diffraction
C-S-H – Calcium Silicate Hydrate
C_2S – belite phase
C_3S – alite phase
AFm – monosulfoaluminate phase
AFt – ettringite phase
CEM II/A-LL 42.5 N – CEM II type cement with a 42.5 MPa compressive strength on day 28
W/B ratio – Water-to-Binder ratio
W/F ratio – Water-to-Filler ratio
W/C ratio – Water-to-Cement ratio
AAC – Autoclaved Aerated Concrete
ECCB – Expanded Clay Cement Block
CBB – Ceramic Building Block
EPS – Expanded Polystyrene
SW – Stone Wool

GENERAL DESCRIPTION OF THE THESIS

Research topicality and problem statement

The construction sector significantly contributes to environmental challenges in Latvia and globally, particularly in the context of the European Union's ambitious climate neutrality goals for 2050 [1,2]. While essential for economic development, the world's construction sector faces mounting pressure to reduce its environmental footprint, especially concerning waste management and resource efficiency. The existing construction and demolition waste (CDW) management practices in Latvia [3], coupled with the sector's substantial carbon footprint, underscores the urgent need for innovative sustainable solutions that align with both national environmental policies [4] and EU directives for the circular economy transition [5].

One tonne of Portland cement is estimated to produce around 0.8 tonnes of CO_2 GHG emissions. Around 8 % of global energy consumption is directly related to the Portland cement production process [6,7]. Consequently, introducing new alternative binder materials in the construction sector is vital for sustainability. Construction and demolition waste are great precursors to introducing new recycling methods and alternative materials to the market. The reactivation of Portland cement-based binders represents a crucial technological frontier in construction material recycling, offering promising pathways for waste reduction and resource optimisation. Current technologies, including mechanical [8], thermal [9], and chemical activation methods [10], demonstrate varying degrees of effectiveness in cement recovery and reuse. However, these processes often remain energy-intensive and economically challenging, highlighting the need for more efficient and sustainable approaches to binder recycling and reactivation [11].

Public perception and market scepticism of recycled building materials regarding their performance and reliability are significant barriers to widespread adoption [3]. Despite testing protocols and quality assurance measures that can validate the mechanical, physical, and durability properties of materials manufactured from secondary resources, these products often face unwarranted stigma in the construction market. This resistance highlights the need for technical innovation and systematic demonstration of performance metrics that meet or exceed industry standards.

The recovery of hardened cement binder from construction and demolition waste streams primarily focuses on concrete and mortar recycling, where effectiveness largely depends on separation methods from aggregates through mechanical, thermal, or chemical processes [12,13]. However, these traditional sources are not the only potential feedstock. Wood-wool cement panels, which typically contain 25–40 % cement binder by weight [14], represent another significant source for cement recovery. Since their introduction in the 1920s, these materials have been widely used throughout Europe for their thermal insulation and acoustic properties. Approximately 174 million m^2 of wood-wool cement panels are expected to be manufactured globally, of which 25 % are manufactured in Europe [15]. This substantial production volume generates considerable manufacturing waste and defective and end-of-life products suitable for cement recovery.

Wood and cement-containing production waste is generated by various processes in their manufacturing stages, such as forming, cutting, processing, and final sorting, where lower-quality materials are separated from higher-quality ones. Recycling end-of-life products is also feasible with the same processing methods as processing production waste. Traditionally, manufacturing waste and end-of-life products are sent to landfills. They can cause pollution, so optimal technologies are being

sought to efficiently recycle these wastes into raw materials (wood-wool and reactivated cement binder) that can be used to produce new building products.

Considering the growing market demand for sustainable construction materials, there remains a critical gap in research regarding the effective recycling and reuse of wood-wool cement panel (WWCP) manufacturing wastes. Often, manufacturing companies do not realise the value of their waste or do not have access to optimal recycling technologies, and the waste is taken to landfills. This research addresses this gap by investigating innovative methods to transform manufacturing and end-of-life waste into viable raw materials usable for producing building materials with lower environmental impact, thereby contributing to waste reduction and resource efficiency in the construction sector.

The aim of the Thesis

This Thesis aims to develop a method for partial separation and recycling of wood-wool cement panel manufacturing and demolition waste into new raw materials for innovative multilayered building panels with a decreased environmental footprint.

Objectives of the Thesis

To achieve the aim, the following objectives are set:

1. **Define** requirements and develop a method for the most effective wood-wool cement board's manufacturing and demolition waste separation into wood and hardened cement paste.
2. **Develop** and **optimise** the method for reactivation of separated hardened cement paste.
3. **Determine** properties of reactivated binder and define the application in the building industry.
4. **Develop** and **characterise** properties of biobased composites for multilayer panels using reactivated binders and production line waste.
5. **Demonstrate** application of multilayered panels in an industrial setting (TRL6).
6. **Validate** the environmental viability of the developed materials by conducting a life cycle assessment and comparison with commercially available products.

The scientific novelty of the research

This research contributes to the circularity of building materials, Green Deal initiatives, and construction industry sustainability. The Thesis aims to develop a method for recycling wood-wool cement panel manufacturing and demolition waste into new raw materials for innovative multilayered building panels with a reduced environmental footprint.

The waste from wood-wool cement panel manufacturing and end-of-life products was collected and analysed. The separation process for hydrated cement paste and wood-wool was optimised. The reactivation of hydrated cement paste through milling and heat treatment techniques was investigated to restore the binding properties of the cement binder.

For the first time, the reactivated Portland-cement-based binders were developed using wood-wool cement panel manufacturing waste and end-of-life products. The separated wood-wool and reactivated cement binder were utilised to create novel biocomposites. These biocomposites, formulated from the

recovered raw materials, demonstrated diverse mechanical and thermal properties. The application of biocomposites (produced from recovered materials) in producing self-bearing multilayered building panels with excellent hydrothermal performance and a reduced environmental impact was demonstrated.

The optimised milling parameters for processing hydrated cement paste effectively fragmented the hydrated cement conglomerates, releasing unhydrated cement minerals. The efficiency, characteristics, and effect of the hydrated cement paste's collision, planetary, and vibration mills were examined. Different reactivated binders were developed by changing the mills' parameters, which allowed obtaining samples with compressive strengths from 0.5 MPa to 15.4 MPa on day 28.

The heat treatment methods proved the reactivation of the cement binder by dehydrating the hydrated minerals. The heat treatment started at around 450 °C when the portlandite started dehydrating. At 600 °C, calcium silicate hydrates (C-S-H) started dehydrating, introducing dehydrated C-S-H products into the reactivated binder, which affected the physical and mechanical properties of the binder.

Cement used in wood-wool cement panel manufacturing typically contains a certain amount of fine limestone. The free lime in the cement clinker and $Ca(OH)_2$, which may form as hydration products in the binder structure, can undergo carbonation over the long service life of recycled wood-wool cement panels. The heat treatment of hydrated cement paste at 900 °C resulted in the decarbonization of $CaCO_3$, but it proved inefficient as it released CO_2 into the atmosphere, which was not the intended outcome. With heating energy emissions and the release of CO_2 from the reaction, the high-temperature heat treatment method is not a sustainable method of reactivation of the cement binder. However, heating below 900 °C proved to be a more sustainable method, scalable to an industrial scale. The reactivated binders proved effective and could be used as a secondary cementitious binder in blended cement, achieving 1.6 MPa to 19.6 MPa compressive strength on the 28th day and lowering the environmental impact of said materials.

The innovation related to improving biocomposites' thermal conductivity involves incorporating a certain amount of hemp shives into the composition. Based on the knowledge gained from the research, novel biocomposites have been developed mainly using production line waste, adding up to 75 % of hemp shives as filler material. Based on their microstructure, hemp shives have proven to be an effective thermal insulator, and their addition to the mix has been proven to decrease the thermal conductivity coefficient.

Developed biocomposites resulted in a self-bearing, low-to-mid density (170–780 kg/m^3) thermal insulation material with a compressive strength of up to 1.4 MPa and a thermal conductivity of 0.052–0.139 W/(m·K). The developed biocomposites have been subjected to an environmental impact assessment and have been found to comply with the EU Green Deal guidelines, lowering the overall emission of 1 m^3 of biocomposite by 26–58 % compared to cement-based alternatives.

Practical relevance of the Thesis

The reactivation of cement binders has been considered a complex, energy-intensive, inefficient process, and many countries do not have standards governing the production and use of reactivated cement in construction. From the perspective of the EU Green Deal, reactivated cementitious binders are an ideal solution to ensure the sustainability of construction processes: reactivated cementitious binders can use industrial by-products and waste as precursors, reducing the consumption of non-

renewable resources and can be produced with reduced environmental impact compared to raw Portland-cement-based binder.

A deeper understanding of the possibilities and advantages of using recycled binders can increase the popularity of the circular approach among professionals in the construction sector. The Thesis describes the results of studies on alternative binders produced from local industrial wastes using either milling or heat treatment, which allows for the efficient disposal of waste products. The results obtained in the Thesis can also be used for pedagogical purposes related to civil engineering, materials science, and chemistry. By transforming approximately 450 000 m^3 of waste into potential raw materials annually, the research offers a tangible solution to industrial waste management. It demonstrates a clear pathway for converting what was once considered waste into valuable, eco-friendly construction materials with potential applications across the construction and manufacturing sectors.

The production of a reactivated binder from industrial by-products allows obtaining a binder with a 28-day compressive strength of up to 20 MPa. Using the developed binders and wood waste as filler, a self-bearing, low-to-mid density (170–780 kg/m^3) thermal insulation material with a compressive strength of up to 1.4 MPa and a thermal conductivity of 0.052–0.139 W/(m·K) was obtained.

Research methodology

Characterising the binder and biocomposites involved several standardised techniques to ensure accurate and reproducible results. For the binder, **granulometry** of sanding dust (waste stream from wood-wool cement panel manufacturing) was performed according to the ASTM C136 standard, using mesh sizes ranging from 0.125 mm to 8 mm. Post-mixing, the developed mortars were placed in a moistened cone on an ASTM C143 impact table, and the **workability** of the mortars was tested.

Material density was calculated mathematically from the dimensions and weight of the samples. **Compressive strength** tests were conducted using a Zwick Z100 universal testing system at a 0.5 mm/min speed. Cubic specimens were measured and weighed to calculate density, which was derived by dividing the mass by the volume. Compressive strength was calculated based on the force applied to the specimen's area. Specimens were dried at 45 °C for 16 hours before testing on days 7, 14, and 28 to remove excess moisture.

Cumulative particle size distribution was analysed using laser diffraction (CILAS 1090), ranging from 0.10 µm to 500.00 µm. **X-ray fluorescence** (XRF) was employed to determine the elemental composition of the samples using a Rigaku ZXS PrimusIV, providing a detailed chemical analysis. **X-ray diffractometric analysis** was performed with a BRUKER-AXS D8 ADVANCE X-ray diffractometer, utilising CuKα1 and CuKα2 radiation in the 2θ range from 10° to 70°. **Thermal properties** were assessed using a Mettler Toledo TGA1/SF thermogravimetric analysis machine, with analyses conducted from 25 °C to 900 °C at 10 °C/min in an air environment.

For biocomposites, **macrostructure and appearance** were evaluated using a Veho HDMI Dual Vision Digital microscope. **Thermal conductivity** was measured with a LaserComp FOX600 heat flow meter according to LVS EN 12667 guidelines, with test settings of 0 °C for the upper plate and 20 °C for the lower plate. The **flexural and compressive strength** tests were conducted using a Zwick Z100 universal testing machine at 0.5 mm/min, following BS EN 12390-3 standards. Compressive strength was measured in both parallel and perpendicular directions to the forming direction, with tests performed until 10 % and 20 % relative deformations in the casting direction and a load of 10 % of the

sample's height for the perpendicular direction. Flexural strength was measured perpendicular to the forming direction for three parallel samples.

Life cycle analysis (LCA) principles were applied to assess the sustainability of binders and biocomposites. The analysis compared 1 kg of binder (developed binders and Portland cement) and biocomposites against commercially available alternatives like rock wool and EPS, maintaining a U-value of 0.18 W/(m²K). Calculations were performed using the SimaPro platform, employing the NE 15804 + A2 V1.03 method as per Product Category Rules (PCR) for building materials.

Limits of research

The research limits can be characterised by the following:

- To obtain a technologically usable sanding dust fraction (**< 0.25 mm**) for reactivation experiments.
- To obtain a reactivated binder with compressive strength of **up to 20 MPa** on day 28 by using the following reactivation methods:
    - collision milling at rotational frequencies of **25** Hz and **50 Hz** for **1 to 5 times**;
    - planetary ball milling with **300 RPM** for the duration of **1 to 30 minutes**;
    - vibration milling for the duration of **5 to 20 minutes**;
    - heating in a muffle furnace **from 300 °C to 1200 °C** for **1 to 5 hours** at the heating rate of **10 °C/min**;
    - heating in a rotary kiln at the speed of **25 RPM** with a **5° inclination** at **450 °C and 900 °C**.
- To obtain biocomposites **as filler using production line waste or a mix of up to 75 % hemp shives**, with a material density of **150–800 kg/m^3**, thermal conductivity coefficient of **0.05–0.15 W/(m·K)**, and compressive strength of up **to 1.5 MPa** on the 28th day after formation.

Theses for defence

- Mechanical activation through optimised milling processes can effectively reactivate partially hydrated cement from wood-wool cement panel manufacturing wastes, producing a low-strength binder of up to 10 MPa on the 28th day, suitable for specific construction applications.
- Heat treatment reactivation at controlled temperatures significantly enhances the binding properties of already hydrated cement-based materials, achieving up to 20 MPa compressive strength compared to mechanical activation.
- Integrating reactivated cement binders with production line waste and hemp shives creates biocomposites that demonstrate comparable thermal insulation and mechanical properties to conventional construction materials while maintaining a low environmental impact.
- The environmental impact assessment of the developed biocomposites confirms their alignment with EU Green Deal objectives, demonstrating a reduced carbon footprint of 26–58 % (47–82 kg CO_2 eq./m^3 of biocomposite). Compared to traditional cement-based products (111 kg CO_2 eq./m^3 of biocomposite).

Composition and scope of the Thesis

The Thesis comprises an annotation in two languages, a general description of the Thesis, nine main chapters divided into sections, conclusions, and a list of references. Chapters 1–3 review the literature and formulate the Thesis's aim and objectives. Chapters 4–7 outline the research methods and materials used and the results obtained through experimental analysis to achieve the objective. Chapter 8 compares the LCA results of the developed materials, and the Conclusions conclude the Thesis.

The thesis comprises of 139 pages, 99 figures, 28 tables, and a reference list with 245 references. The thesis is written in English.

Approbation of the Thesis results

Participation in conferences. The key findings and methodological innovations have been shared and reviewed at international scientific conferences, allowing for expert opinion and feedback.

1. Riga Technical University 62nd International Scientific Conference, Section "Civil Engineering," Riga, Latvia, 28.10.2021.
2. 5th International Conference "Innovative Materials, Structures and Technologies" IMST 2022, Riga, Latvia, 28–30.09.2022.
3. Riga Technical University 63rd International Scientific Conference, Section "Civil Engineering," Riga, Latvia, 10.11.2022.
4. XVI International Scientific conference of environmental and climate technologies "Conect 23", Riga, Latvia, 10–12.05.2023.
5. 5th International Conference on Bio-Based Building Materials "ICBBM 2023", Austria, Vienna, 21–23.06.2023.
6. Riga Technical University 64th International Scientific Conference, Section "Civil Engineering," Riga, Latvia, 19.10.2023.
7. XVII International Scientific Conference of Environmental and Climate Technologies "Conect 2024", Riga, Latvia, 15–17.05.2024.
8. The 4th International Conference on Sustainable Development in Civil, Urban and Transportation Engineering "CUTE 2024", Wroclaw, Poland, 14–16.10.2024.
9. 6th International Conference on Bio-Based Building Materials "ICBBM 2025", Rio de Janeiro, Brazil, 17–20.06.2025.

Academic Publications. The research has been presented in four conference proceedings and five publications in scientific journals indexed in the SCOPUS database; in total, they have been cited 83 times, h_5-index – 5 (h-index – 6). The research has been published in such international journals as *Recycling*, *Environmental and Climate Technologies*, and *Materials*.

Industrial Collaboration. The research was conducted in close collaboration with Cewood®, a leading producer of wood-wool cement panels, ensuring practical relevance and real-world applicability of the developed methods and materials.

List of publications

1. **Argalis, P. P.**; Sinka, M.; Bajare, D. Recycling of Cement-Wood Board Production Waste into a Low-Strength Cementitious Binder. *Recycling* 2022, *7*, 76, doi:10.3390/recycling7050076.
2. **Argalis, P. P.**; Sinka, M.; Bajare, D. A Preliminary Study of Mechanical Treatments' Effect on the Reactivation of Hydrated Cement Paste. *J. Phys. Conf. Ser.* 2023, *2423*, 012008, doi:10.1088/1742-6596/2423/1/012008.
3. Bumanis, G.; **Argalis, P. P.**; Sahmenko, G.; Mironovs, D.; Rucevskis, S.; Korjakins, A.; Bajare, D. Thermal and Sound Insulation Properties of Recycled Expanded Polystyrene Granule and Gypsum Composites. *Recycling* 2023, *8*, 19, doi:10.3390/recycling8010019.
4. **Argalis, P. P.**; Bumanis, G.; Bajare, D. Gypsum Composites with Modified Waste Expanded Polystyrene. *Journal of Composites Science* 2023, *7*, 203, doi:10.3390/jcs7050203.
5. **Argalis, P. P.**; Sinka, M.; Andzs, M.; Korjakins, A.; Bajare, D. Development of New Bio-Based Building Materials by Utilising Manufacturing Waste. *Environmental and Climate Technologies* 2024, *28*, 58–70, doi:10.2478/rtuect-2024-0006.
6. Bumanis, G.; **Argalis, P. P.**; Sinka, M.; Korjakins, A.; Bajare, D. The Use of Recycled Cement-Bonded Particle Board Waste in the Development of Lightweight Biocomposites. *Materials* 2024, *17*, 5890, doi:10.3390/ma17235890.
7. **Argalis, P. P.**; Sinka, M.; Bumanis, G.; Bajare, D. Application of a Recovered Low-Strength Binder from Wood–Cement Particleboard Production. *In Proceedings of the 4th International Conference on Sustainable Development in Civil, Urban and Transportation Engineering*; Springer, 2025; Vol. 418, pp. 245–253.
8. Hajj Obeid, M.; **Argalis, P. P.**; Sinka, M.; Bajare, D.; Pailha, M.; Woloszyn, M. Advancing Sustainable Building Technologies: A Focus on Bio-Based Multi-Layer Panels and Real-Scale Hygrothermal Analysis. In *Proceedings of the 4th International Conference on Sustainable Development in Civil, Urban and Transportation Engineering*; Springer Nature, 2025; Vol. 418, pp. 323–332.
9. **Argalis, P. P.**; Puzule, L.; Sinka, M.; Bajare, D. Transforming Cement-Wood Fiber Industrial Byproducts into Hybrid Binder. In: *Bio-Based Building Materials – Proceedings of ICBBM 2025*; Springer Nature, 2025; pp. 738–751, doi:10.1007/978-3-031-92874-1_58.
10. Balina, K.; Gailitis, R.; Sinka, M.; **Argalis, P.P.**; Radina, L.; Sprince, A. Prospective LCA for 3D-Printed Foamed Geopolymer Composites Using Construction Waste as Additives. Sustainability 2025, 17, 6459, doi:10.3390/su17146459.

1. ENVIRONMENTAL IMPACT AND CLIMATE STRATEGIES IN LATVIA

The construction materials sector significantly impacts global resource consumption and environmental sustainability. It accounts for 33 % of energy-related CO_2 emissions. Material consumption is a major concern, with construction materials representing about 50 % of all raw materials extracted globally [16]. Concrete production contributes about 8 % of global CO_2 emissions, and the steel industry, heavily linked to construction, accounts for roughly 9 % [17]. Concrete production consumes around 10 % of the world's industrial water [18].

Latvia's construction sector is vital to its economy, contributing significantly to the national GDP and employing a substantial workforce [19]. Latvia's extensive forest coverage makes timber a key construction material, raising sustainability issues regarding forest management [20]. There is also pressure from mineral extraction, with sand, gravel, limestone, and clay extraction impacting the environment [21]. Water quality is also affected by construction activities [22].

Latvia is part of the European Union's climate neutrality plan, which aims for net-zero greenhouse gas emissions by 2050 [23]. The EU is targeting a 55 % reduction in embodied carbon emissions by 2030 and 100 % by 2050, alongside promoting circular economy practices to manage construction and demolition waste (CDW) [24]. Latvia has committed to a 65 % reduction in greenhouse gas emissions by 2030 compared to 1990. It is working to reduce energy consumption in new buildings and renovate public buildings for better energy efficiency [25].

Latvia's regulatory framework includes the Construction Law, Energy Efficiency of Buildings Law, and Public Procurement (GPP) regulations to promote sustainable construction [26]. Challenges include coordination between authorities, enforcement inconsistencies, and the need for a holistic approach to sustainability [27].

Latvia's construction sector generates a significant amount of waste [28]. The country's waste management framework, guided by EU directives, prioritises prevention, reuse, recycling, and recovery [29]. CDW is classified, with disposal fees varying. Challenges to circular CDW management include market issues, regulatory shortcomings, and citizen behaviour. Solutions involve government initiatives, market opportunities, and citizen engagement, including urban recycling centres [30].

With the increased adoption of international frameworks, sustainability assessment in Latvia's construction sector is evolving [31]. Economic, social, and environmental factors are considered. Life cycle assessment (LCA) is a key tool for evaluating environmental impact [32].

2. WOOD-WOOL CEMENT PANELS

Wood-wool cement panels are made from spruce wood, chosen for its uniform cross-section. The wood is peeled, pruned, and dried on elevated surfaces for 6 to 12 months to ensure proper moisture migration. During this drying period, resins and sugars in the wood migrate to its surface [33]. The dried timber is cut into 50 cm blocks, the optimal size for manufacturing. Larger blocks are split, and offcuts are used for energy recovery. The blocks are placed on racks, ensuring a mix of wood to minimise dispersion during manufacturing. Moisture content is measured from sample blocks at the start of each shift, and this data is recorded. Water is added during manufacturing, and adjustments are made based on the wood's density. The blocks are shaved into wood fibres, which are then moistened.

The wood wool is mixed with cement, and the ratio can be adjusted. The first stream of waste material (production line waste) is produced before the mixture reaches rotary dispersers and is collected at the end of the shift to be sent to a landfill. The mixture is fed into moulds, smoothed, and laid in two layers. Cement curing times vary, and adjustments are made to maintain quality. The panels are pressed, cut to 2.4 m lengths, and stacked for curing. Temperature is monitored during this process to prevent scorching. After curing, the panels are demoulded, milled, and sawn. This process generates additional waste. The panels are then moved to a second warehouse for further drying, which takes approximately 2–4 weeks. The drying process has been optimised to reduce drying time.

Dried panels undergo quality control, where they are sanded, milled, and visually inspected. Sanding produces sanding dust, which is collected to avoid respiratory risks [34]. Defective panels, comprising 3–5 % of production, are mainly used for pallet material to reduce the dents of newly produced panels. The finished panels are stored in a warehouse before being transported.

Wood-wool cement panels are used for both acoustic and construction purposes. Acoustic panels are used in interiors for sound insulation and noise absorption in offices, schools, and music halls. Construction panels are used in construction, insulation, and sound insulation [35].

The manufacturing process uses spruce wood, white or grey cement, industrial water, and water-based varnishes and colours. The process generates several waste streams, including production line waste, sawing waste, and sanding dust. There is potential to use the waste to develop biocomposites, utilising coarse wood-wool waste and modified sanding dust. The longer wood fibres can provide mechanical interlocking, and the sanding dust can act as a binder. This approach aims to create sustainable and economically viable biocomposites.

3. REACTIVATION OF PORTLAND CEMENT-BASED BINDERS

As the demand for sustainable materials grows, researchers increasingly focus on the reactivation and recycling of Portland cement-based binders, particularly from cement-based production waste [36,37]. This multifaceted technological approach aims to revive the binding properties of partially hydrated cementitious materials, transforming waste into valuable construction resources [38,39]. By implementing advanced reactivation technologies, the industry can address significant environmental concerns such as waste generation, resource depletion, and carbon emissions [6].

Mechanical activation through milling processes significantly enhances cement reactivity by reducing particle sizes from 10–50 μm to less than 5 μm, increasing specific surface area, and introducing lattice strain and structural defects that accelerate chemical interactions [40]. Three primary milling techniques – planetary ball milling, collision milling, and vibratory milling – demonstrate unique capabilities in modifying material characteristics [41–43]. However, challenges remain regarding energy consumption, equipment wear, and potential particle agglomeration.

Heat treatment represents another effective reactivation strategy, utilising various techniques, including pyrolysis, calcination, and incineration, to modify cement stone's physical and chemical properties [44]. Muffle furnaces, with their enclosed heating chambers and precise temperature control (typically 400–900 °C), are ideal for laboratory-scale investigations, while rotary kilns offer advantages for continuous operation and industrial-scale processing [45]. Microwave heating has shown promise, with studies demonstrating up to 30 % increases in compressive strength compared to untreated samples due to selective molecular vibration and dielectric heating processes [46].

Milling technologies can increase CO_2 emissions by around 30–50 % compared to conventional cement production due to the higher energy consumption [47]. Heat treatment must address scalability and economic feasibility [39]. Initial equipment costs for advanced heating technologies range from 250,000 to € 1.5 million [48]. Chemical processing can reduce raw material consumption by 25–35 % [49], but costs are around 150–300 €/t of processed cement [50], and there is a potential risk of chemical waste and water pollution. Well-designed reactivation processes can reduce material procurement costs by 20–40 % compared to conventional production [51].

4. MATERIALS AND METHODS

4.1. Raw Materials

Sanding Dust (SD)

In the final manufacturing stage of wood-wool cement panels, cured and dried panels undergo cutting, edge treatment, and size calibration through sanding. A dust extraction system minimises dust and maintains a clean work environment to mitigate potential health risks from airborne dust exposure during sanding. The continuous grinding and filter-cleaning processes produce about 4–5 m^3 of SD daily. The SD primarily consists of two key components: wood fibre particles and partially hydrated cement particles. Wood fibre particles are typically elongated and fibrous, resembling strands.

In contrast, cement particles are usually much finer, appearing as small, irregularly shaped grains or fragments. Cement particle morphology is influenced by cement type, fineness, and hydration state.

The SD originates from sanding the wood-wool cement panels after 3 to 4 weeks of hardening. 72 wt.% of sawing dust is smaller than 0.25 mm; therefore, hydrated cement's fine nature and high content could be used as supplementary cementitious material or as a material for reactivation and production of new binder.

Fine particles from SD are proposed as raw materials for developing binders to make biocomposites with production line waste (PLW) as filler. Binder recovery was examined through two different approaches:

1. Mechanical reactivation with three different milling methods.
2. Heat treatment from 300 °C to 1200 °C in a muffle furnace and 450 °C and 900 °C in a rotary kiln.

Production Line Waste (PLW)

This research used production line waste (PLW) as the bio-based aggregate for biocomposites. The material is spruce wood fibres ranging from 5 mm to 200 mm in length, from 1 mm to 1.5 mm in width and from 0.5 mm to 0.8 mm in thickness. The average bulk density is 250 kg/m^3. The wood fibres are coated with hydrated cement from the manufacturing process. Most of the fibres have been separated from one another, except for small patches of fibres that have clumped together. The bio-based aggregates are checked before the sample preparation to avoid these hardened patches of material for a more homogenous structure. The visual appearance of the material can be observed in Fig. 4.1.

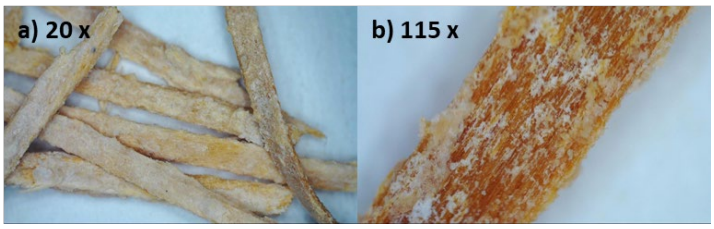

Fig. 4.1. The visual appearance of PLW at different magnifications.

Other Materials

Other materials include CEM II/A-LL 42.5 N and hemp shives. This type of cement (Schwenk, Latvia) is produced by blending ordinary Portland cement clinker (80–94 %) with limestone as a secondary constituent. The limestone component typically comprises 6–20 % of the cement composition. The rest are minor additional constituents, resulting in 0–5 % of the total cement composition [52]. Natural Fibre (Natūralus Pluoštas, Lithuania) produced hemp shives were utilised as additional bio-based aggregates to lower the thermal conductivity coefficient, as their thermal conductivity is 0.043 W/(m·K). The hemp shives supplied by this regional processor are the only ones suitable for making building materials. 64 % of the hemp shive particles range from 1 mm to 20 mm. The shives have an 80 kg/m^3 bulk density and a 115 kg/m^3 compacted bulk density [53].

4.2. Modification of the Sanding Dust

Sanding dust was sieved according to the process depicted in Section 4.1. The sieved fraction below 0.2 mm was used as the binder precursor and processed in three mechanical mills and two heat treatment methods. For the investigation of the effect of milling on binder quality, sieved sanding dust was subjected to mechanical processing of:

- collision milling using Desi Desi-16C (Estonia, 2016) at 25 Hz and 50 Hz frequencies for 1, 3, and 5 milling cycles);
- planetary ball milling using Retsch PM 400 (Germany, 2007) of 1 to 30 minutes at 300 RPM;
- vibration milling using Stankomash MV-20 (Russia, 2016) for 5, 10, 15, and 20 minutes.

Assessing different reactivation mechanisms, sieved sanding dust was subjected to heat treatment using two methods:

- heating in Uterna W-80 muffle furnace (Lithuania, 2012) for 1 to 5 hours at 300 °C, 450 °C, 600 °C, 750 °C, 900 °C, 1050 °C, and 1200 °C at the heating rate of 10 °C/min;
- heating in Keramserviss KLR rotary kiln (Latvia, 2009) at 450 °C and 900 °C at 5° at 25 RPM.

Altogether, 37 different binders were developed using 5 processing methods. Each binder is characterised in the respective Thesis chapter.

4.3. Characterisation Techniques

Granulometry of sanding dust was performed according to ASTM C136 [54] standard with a mesh size of 0.125 mm to 8 mm.

The flowability of the mortars was tested on an EN 1015-3 impact table. The diameter and height of the cone were also measured. Twenty jolts were performed with the impact table, and the reaction of the mortar to this force was observed. The cone's diameter was measured, and the cone's flowability was analysed.

The compressive strength was tested using a Zwick Z100 universal testing system (ZwickRoell, Kennesaw, GA, USA) at a 0.5 mm/min test speed. The samples were dried at 45 °C for 16 hours before testing to remove excess water from the structure, and were tested on days 7, 14, and 28.

Cumulative particle size distribution of the materials obtained by laser diffraction (CILAS 1090, range 0.10–500.00 μm).

X-ray fluorescence (XRF) is a widely used analytical method for determining the elemental composition of a sample. The XRF was performed on a Rigaku ZXS PrimusIV.

X-ray diffractometric (XRD) analysis of the material was carried out using a BRUKER-AXS D8 ADVANCE X-ray diffractometer (Bruker, Billerica, MA, USA) using CuKα1 and CuKα2 radiation in the 2θ range from 10° to 70°.

The physical properties of the temperature effect on the raw materials were determined using a Mettler-Toledo TGA1/SF thermogravimetric analysis machine. At the same time, Mettler STARe software helps to obtain thermograms through which mass changes and release of destruction products can be determined. The mode used for the analyses is 25–900 °C at 10 °C/min in an air environment.

Biocomposites were characterised using a digital microscope, Veho HDMI Dual Vision Digital, to assess the biocomposites' macrostructure and visual appearance.

Thermal conductivity was measured with a LaserComp FOX600 heat flow meter; according to the standard LVS EN 12667 guidelines, the test settings were 0 °C for the upper and 20 °C for the lower plate.

The compressive and flexural strength of the bio-based building materials was tested at 0.5 mm/min using Zwick Z100 universal testing equipment (ZwickRoell, Kennesaw, GA, USA) according to BS EN 12390-3 and LVS EN 826 standard.

4.4. Life Cycle Assessment

The environmental evaluation of the developed materials was conducted using the life cycle assessment (LCA) approach. Calculations were performed in SimaPro with the Ecoinvent 3.8 database. The primary goal was to compare the biocomposites made with existing insulation materials based on their thermal insulation properties. The functional unit was chosen for biocomposites to compare their thermal insulation effectiveness based on the U-value of 0.18 W/(m²·K) per m^2 of either biocomposite or wall assembly.

Comparisons were made with traditionally used building materials. Life cycle assessment results for these materials were taken from previous studies and adapted to match the functional unit used in this study [55]. To compare developed biocomposites with traditional building materials, a wall assembly with a wooden frame was made (see Table 4.1). The approximate thickness of the wall assembly is 36–39 cm.

Table 4.1

Wall Assembly Input Data

Material	Thickness, mm	Amount, kg
Wooden frame	–	6.3
Spun planks	25	17.5
Developed insulation material	257–280*	92.4–122.1*
Frontrock wool	30	1.8
Anti-wind film	–	–
Wood-wool cement panel	50	21.0

* Depending on the binder type in the biocomposite.

5. MILLING EFFECT ON THE REACTIVATION OF THE SANDING DUST

5.1. Sanding Dust Reactivated by Planetary Ball Mill

Mix Design and Sample Preparation

In this experiment, sanding dust (SD) was processed using a planetary ball mill to investigate its potential as a binder in mortar compositions. Eleven compositions were created, including two reference samples. The water-to-binder (W/B) ratio was adjusted for each sample to achieve a 15–20 cm flowability after 20 revolutions on an impact table. The required amount of SD and water was mixed. The mixed material was formed in moulds (20 mm × 20 mm × 20 mm), covered in plastic film and left to cure at ambient conditions (atmospheric pressure, 20 ± 2 °C) for 2 days; flowability and setting times were measured according to EN 196-3. Samples were cured in sealed plastic bags to maintain high humidity. Compressive strength was tested at 7, 14, and 28 days. For each testing time, six replicate samples were tested to obtain more reliable results.

Results

The results showed that milling the SD affected the material's properties. Increasing milling time influenced the workability and setting time of the material. For example, mortars made with SD milled for 1 minute showed good workability, and increasing milling time to 10 minutes further improved workability. However, excessive milling times decreased workability. Setting times varied with milling duration, with SD milled for 10 minutes, setting the fastest.

Compressive strength generally increased with milling time, with the highest strength observed in samples milled for 15 minutes. However, milling beyond 15 minutes did not significantly increase strength (Fig. 5.1).

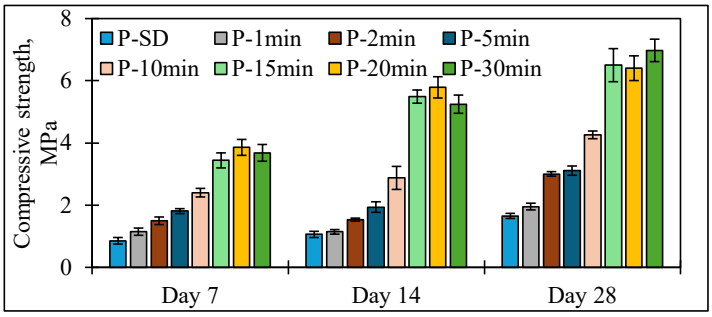

Fig. 5.1. Summary of compressive strength results for the planetary ball milling method.

The study concluded that milling SD in a planetary ball mill improves compressive strength and workability. The optimal processing parameters identified were 15 minutes of milling with a W/B ratio between 0.6 and 0.8 and curing in high-humidity conditions.

5.2. Sanding Dust Reactivated by Collision Milling

Mix Design and Sample Preparation

This section explores the use of sanding dust processed in a collision mill as a binder. Seven compositions were created, varying in processing frequency (25 Hz and 50 Hz) and number of processing cycles (1, 3, and 5). A reference sample series was also included. All compositions used a W/B ratio of 0.7. Samples (20 mm × 20 mm × 20 mm) were cured in a high-humidity environment (20 ± 2 °C, RH > 90 %) for 5 days, then demoulded and cured at room temperature in a plastic bag to retain moisture. Compressive strength was measured at 7, 14, 28, 90, and 180 days. For each testing time, 4–5 replicate samples were created to obtain more reliable results.

Results

The results indicated that compressive strength improved over time for all samples (Fig. 5.2). As time progressed, there was a consistent increase in compressive strength across all samples. By day 14, compressive strength increased slightly to around 0.8–1.0 MPa; by day 28, it reached approximately 1.5 MPa. The strength development continued significantly, reaching about 2.5–3.0 MPa by day 90.

The most remarkable strength development occurred between days 90 and 180, where all samples showed substantial increases in compressive strength. Interestingly, on day 180, there was a notable differentiation between processing conditions. The D-3x-50Hz and D-5x-50Hz demonstrated higher compressive strengths at around 4.9–5.0 MPa compared to their 25 Hz counterparts (D-3x-25Hz and D-5x-25Hz), reaching 3.6–3.8 MPa. The D-SD sample reached 3.9 MPa on day 180, showing that milling at 25 Hz is insufficient to propose any enhancement to compressive strength.

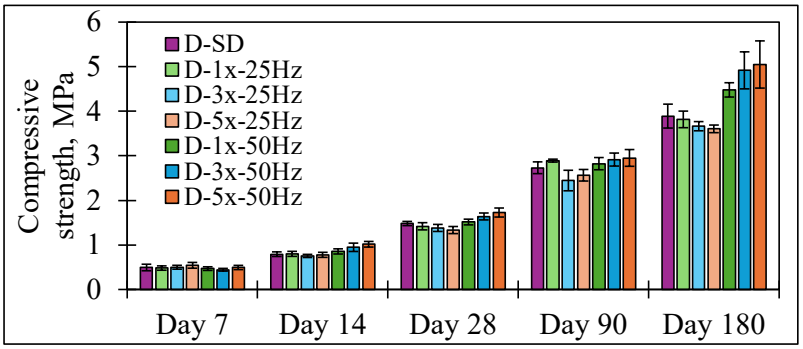

Fig. 5.2. Compilation of the compressive strength.

The role of processing frequency (25 Hz vs 50 Hz) becomes more pronounced at later stages. By day 180, the 50 Hz processed samples show higher compressive strengths than the 25 Hz samples. This could indicate that SD processed at a higher frequency might lead to better particle distribution or more efficient reactivation of the partially hydrated cement in the SD. The multiple processing cycles (3 and 5 times) at 50 Hz enhance this effect.

From a materials science perspective, this behaviour might be explained by several mechanisms:

- the increasing strength suggests retarded but continued cement hydration processes and better bonding between wood particles and cement over time;
- the higher frequency processing (50 Hz) creates a more optimal particle size distribution or exposes more surface area [56,57] of the partially hydrated cement for new hydration reactions [58].

The D-SD shows moderate performance in compressive strength, suggesting that mechanical processing in low frequencies does not influence the material's properties.

5.3. Sanding Dust Reactivated by Vibration Mill

Mix Design and Sample Preparation

This experiment examined sanding dust processed in a vibration mill as a binder. Four compositions with varying milling durations and one reference composition were created. A W/B ratio of 0.8 was used for all samples (20 mm x 20 mm x 20 mm). Workability and setting times were measured, and samples were cured for 5 days (20 ± 2 °C), followed by further curing in sealed bags. Compressive strength was tested at 7, 14, and 28 days.

Results

Flowability results indicated that all the mortars are workable using a W/B ratio of 0.8. Increasing the milling time of SD to 20 minutes reduces the workability of the material.

Summarising the compressive strength results (Fig. 5.3), there is an increase in compressive strength with increasing milling time. Figure 5.6 shows the compressive strength data. The lowest compressive strength was obtained for V-SD, achieving 0.8 MPa on day 28. Marginally close V-5min achieved 0.9 MPa. Sample V-15 min achieved 1.4 MPa; the highest compressive strength was obtained for the V-20min, reaching 1.6 MPa on day 28. From these results, it can be concluded that increasing the milling time of SD can increase the compressive strength of the mortars.

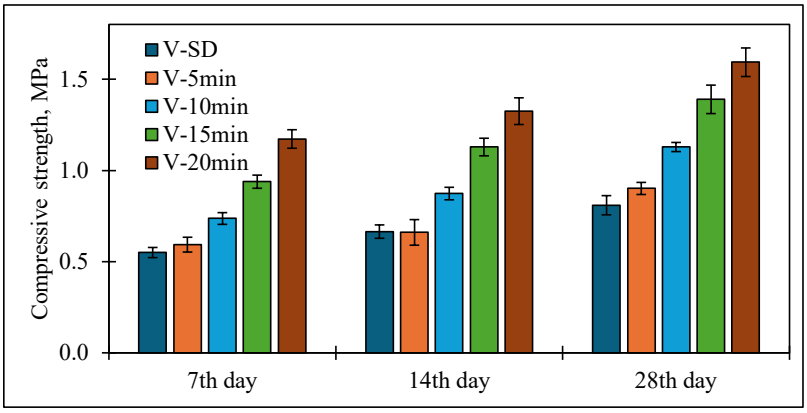

Fig. 5.3. Summary of compressive strength results for the vibratory milling method.

The compressive strength differences remain significant and even appear to widen slightly with time. This suggests that more prolonged milling continues to influence strength development persistently.

5.4. Chapter Summary

The research investigated the reactivation of sanding dust through different milling methods.

Planetary ball milling demonstrated that high-humidity curing conditions yielded the best compressive strength results. Milling duration significantly impacted workability and compressive strength, achieving 7.0 MPa on the 28th day for SD milled for 30 minutes.

Collision milling improved compressive strength, with higher processing frequencies leading to better results at later stages. However, the strength gain was not energy-efficient, as it achieved 1.7 MPa on the 28th day.

Vibration milling showed that milling duration influences workability and compressive strength, offering a more scalable approach, reaching 1.6 MPa on the 28th day.

Comparing the three methods, planetary ball milling achieved the highest strength but had limited scalability. Collision milling had moderate strength gains but poor energy efficiency. Vibration milling provided a balance of performance, energy efficiency, and scalability.

6. HEAT TREATMENT EFFECT ON THE REACTIVATION OF THE SANDING DUST

6.1. Sanding Dust Reactivated by Heating in Muffle Furnace

The heat treatment aimed to characterise the heat-treated SD mortar properties in raw and hydrated states to understand if this processing method has potential. Temperature was chosen in increments of 150 ℃, starting from 300 ℃ to 1200 ℃, holding the selected temperature for four hours. Four hours was considered sufficient time to heat the entire batch of material. The temperatures were chosen based on studies available in the literature [59,60] and the results of the previous phase.

Mix Design and Sample Preparation

The mix designs are detailed in Table 6.1. Seven temperature-based compositions were created with a corresponding reference sample (M-SD-2) for sanding dust (SD) composition variations. The heat-treated SD was used as a binder. Different water-to-binder (W/B) ratios were used to achieve consistent workability across samples. One mass part of the proposed binder was used for each composition.

Table 6.1

Mix Design for Samples

Sample	M-SD-2	M-300-2	M-450-2	M-600-2	M-750-2	M-900-2	M-1050-2	M-1200-2
Water, according to EN 196-3, mass parts	0.70	0.60	0.73	0.60	0.65	0.65	0.70	0.25

Samples were prepared using a Hubert automatic mixer at 140 RPM. 500 g of material was mixed with water (according to EN 196-3 standards) for 2 minutes, followed by manual stirring and an additional 2–3 minutes of mixing until homogeneous. The resulting mortar was moulded into Vicat apparatus rings and 20 mm × 20 mm × 20 mm moulds, which were then covered with plastic film. After a two-day initial curing period, samples were demoulded, labelled, and stored in sealed plastic bags for continued curing. Three parallel samples were tested on each testing day.

Results

The thermal behaviour of wood-wool cement panel sanding dust shows complex decomposition patterns of both lignocellulosic and cementitious materials. Thermogravimetric (TG) analysis (300–900 ℃) reveals multiple mass loss stages, with corresponding DTA curves showing thermal events attributed to specific transformations (Fig. 6.1). The initial dehydration stage (50–150 ℃) shows ~ 10 % mass loss, primarily from the evaporation of bound water [61,62], including adsorbed water from wood fibres [62,63], interlayer water from C-S-H gel [64], zeolitic water from AFm phases [65] and ettringite dehydration (90–120 ℃) [66]. The endothermic DTA character confirms these processes' dehydration nature.

The intermediate temperature region (150–400 °C) exhibits a gradual mass decline corresponding to the thermal degradation of wood components [67–69]. This begins with hemicellulose decomposition (220–315 °C) [67,69–71], followed by cellulose degradation initiation (315–400 °C) [67,70,72]. Lignin decomposition occurs gradually across a broad temperature range (200–500 °C) [62,66,67,69,71,73]. The cement phases also contribute to mass loss in this region through the dehydration of ettringite (AFt) around 120 °C and monosulfoaluminate (AFm) phases between 180–200 °C [74].

A distinctive endothermic event occurs around 450 °C, accompanied by a mass loss step, indicating the dihydroxylation of $Ca(OH)_2$ (Portlandite): $Ca(OH)_2 \rightarrow CaO + H_2O$. This reaction is fundamental in cement chemistry and affects the material's subsequent carbonation behaviour [61,62,66–71,73,75–78].

The most pronounced endothermic peak appears at approximately 750 °C, coinciding with a sharp 10–15 % mass loss, representing the decarbonisation of calcium carbonate: $CaCO_3 \rightarrow CaO + CO_2$. The presence of $CaCO_3$ suggests either carbonation of $Ca(OH)_2$ during material processing/storage or limestone in the original cement composition [79]. The carbonation process in cement-based materials follows the reaction: $Ca(OH)_2 + CO_2 \rightarrow CaCO_3 + H_2O$. This process is particularly relevant for fine particles like sanding dust due to their high surface area [61,62,66,68,69,71,73,76–78,80].

The heat-treated SD (300–900 °C) demonstrates progressively reduced mass loss at lower temperatures, confirming the irreversibility of thermal decomposition processes. However, the persistence of some thermal events in pre-heated samples suggests several possibilities:

1) incomplete reactions during initial heating due to kinetic limitations [81];
2) reformation of hydrates and carbonates during cooling/storage [82];
3) protection of some phases within the composite matrix [83].

The final residual mass between 70–95 % provides quantitative information about the total volatile and decomposable content, reflecting the combined effects of dehydration, dihydroxylation, and decarbonisation processes [84]. Heat treating SD to above 750 °C resulted in a small fraction of portlandite phase reforming during the cooling or storage process [85,86].

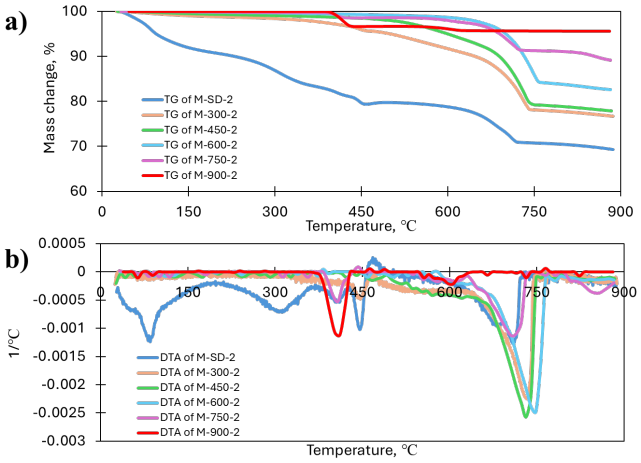

Fig. 6.1. a) TG, b) DTA curves for the samples.

The physical and mechanical properties of the materials were also re-investigated after the results of the first phase. The materials' elemental distribution and mineralogical composition were determined in cooperation with the cement manufacturer SCHWENK and their laboratory. The data on the elemental distribution are summarised in Table 6.2. As the temperature increases, the material undergoes phase changes and decomposition reactions, further explained by the TG/DTA graph shown in Fig. 6.1.

The XRF data provided in Table 6.2 reveal significant changes in the oxide composition of wood-wool cement panel manufacturing waste as it was heated from 0 °C to 1200 °C. The most notable change is the substantial increase in CaO content from 51.11 % to a peak of 68.84 % at 1050 °C, due to the decomposition of calcium-containing compounds such as calcium carbonates from hydrated cement, as can be seen from TG/DTA data in Fig. 6.11. Simultaneously, there is a decrease in CO_2 content from 25.12 % to 2.26 % at 1050 °C, further indicating the breakdown of carbonates. The similar amounts of CO_2 after 900 °C indicate that all carbonates have decomposed, and the remaining CO_2 is crystalline-bonded CO_2. SiO_2 gradually increases from 17.02 % to 22.05 %, possibly resulting from the decomposition of calcium silicate hydrates in cement and the oxidation of silicon-containing compounds in wood. Al_2O_3 content rises slightly from 2.49 % to 3.13 % due to the dehydration of aluminium-containing phases in the cement.

Table 6.2

Oxide Distribution of Elements

Sample	SiO_2	Al_2O_3	Fe_2O_3	CaO	MgO	SO_3	Na_2O	K_2O	TiO_2	Mn_2O_3	P_2O_5	Cl	CO_2	Na_2O eq
M-SD-2	17.02	2.49	0.60	51.11	1.70	1.33	0.16	0.16	0.10	0.17	0.03	0.03	25.12	0.26
M-450-2	18.28	2.72	0.67	56.96	1.79	1.56	0.19	0.19	0.11	0.17	0.03	0.03	19.72	0.31
M-600-2	18.95	2.70	0.64	59.08	1.76	1.53	0.19	0.16	0.10	0.19	0.03	0.02	16.71	0.30
M-750-2	20.01	2.91	0.68	63.60	1.81	1.56	0.19	0.17	0.11	0.19	0.04	0.02	8.70	0.30
M-900-2	21.53	3.00	0.68	67.66	1.86	1.64	0.19	0.16	0.12	0.21	0.04	0.02	3.75	0.29
M-1050-2	21.97	3.04	0.70	68.84	1.87	1.33	0.14	0.09	0.12	0.22	0.04	0.02	2.26	0.19
M-1200-2	22.05	3.13	0.70	67.65	1.88	1.23	0.10	0.06	0.12	0.22	0.04	0.01	3.19	0.14

Other oxides like Fe_2O_3, MgO, and minor components show relatively small changes throughout the heating process. SO_3 increases slightly up to 900 °C before decreasing at higher temperatures, suggesting the decomposition of sulphate-containing phases [87]. Alkali oxides (Na_2O and K_2O) show slight increases up to 750 °C, due to the concentration effects as other components degrade and then decrease due to volatilisation at high temperatures in the cement matrix [88]. These changes indicate the dehydration and decomposition of hydrated cement phases, breakdown of carbonates, and formation of calcium, silicon, and aluminium oxides typical of cement clinker as the temperature increases.

This data is further explained by the XRD results, shown graphically in Figs. 6.2 and 6.3. The XRD analysis of the wood-wool cement panel sanding dust provides a comprehensive picture of the complex mineralogical transformations occurring as the material is subjected to increasing temperatures. This analysis is crucial for understanding the material's behaviour and potential applications in recycling or reuse strategies.

At room temperature, the M-SD-2 composition reflects the containing carbonates and the carbonation process that occurs during the lifecycle of cement-based materials. Calcite ($CaCO_3$) is the predominant phase, indicating carbonation of the cement phases. This is a common phenomenon in

cement-based materials exposed to atmospheric CO_2 over time [89]. Small amounts of portlandite ($Ca(OH)_2$) also represent the remaining hydration products. Heat treating SD to above 750 °C resulted in a small fraction of portlandite phase reforming during the cooling or storage process [85,86].

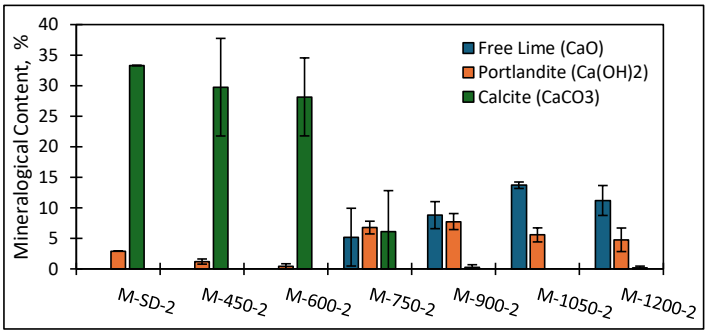

Fig. 6.2. Summary of the mineralogical content of free lime, portlandite, and calcite.

We observe decomposition reactions and phase transformations as the temperature increases. The portlandite decomposes around 450–600 °C, converting to calcium oxide and water vapour. This aligns with the findings of Alarcon-Ruiz et al. [90], who noted this decomposition occurring typically between 400–500 °C in cement pastes.

The most dramatic change occurs with the thermal decomposition of calcite, which begins around 600–700 °C and is essentially complete by 750 °C. This process, represented by the reaction $CaCO_3 \rightarrow CaO + CO_2 \uparrow$, is responsible for the significant mass loss observed in this temperature range. This decomposition's kinetics and exact temperature can vary based on particle size, heating rate, and CO_2 partial pressure in the environment [91].

Concurrently with these decomposition processes, the cement clinker phases (C_3S and C_2S) undergo significant transformations. The behaviour of alite (C_3S) and the various polymorphs of belite (C_2S) are particularly noteworthy. Alite content decreases with increasing temperature, likely due to its thermal instability and potential reaction with decomposition products. While pure alite typically decomposes around 1250 °C, in complex systems like this, it can begin to transform at lower temperatures [92].

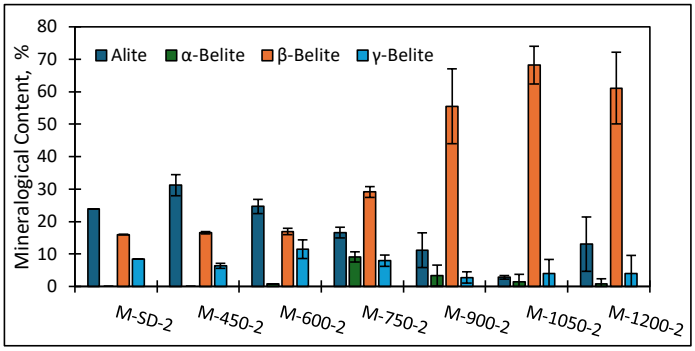

Fig. 6.3. Summary of the mineralogical content of the alite and belite phases.

The belite phases exhibit a series of polymorphic transformations critical to understanding the material's evolving properties. The conversion of γ-C_2S to β-C_2S, becoming dominant above 725 °C,

is a key transition. This transformation is significant because β-C_2S is more reactive than γ-C_2S, potentially enhancing the hydraulic activity of the thermally treated dust [93]. The appearance of small amounts of α-C_2S at higher temperatures (above 750 °C) is intriguing and may be due to the stabilisation of this high-temperature polymorph by impurities or specific cooling conditions [94]

These phase transformations have important implications for the potential reuse of the material. The increase in reactive phases like β-C_2S at higher temperatures suggests that thermal treatment could enhance the cementitious properties of the SD. This aligns with research by Shui et al. [79], who found that dehydrated cement pastes can regain hydraulic activity, potentially serving as a supplementary cementitious material.

Another critical aspect is the presence and evolution of free lime (CaO) with increasing temperature (> 900 °C). While some free lime benefits cement reactivity, excessive amounts can lead to expansion and durability issues in hardened cement-based materials. Therefore, carefully considering the optimal treatment temperature is necessary to balance the formation of reactive phases with the potential risks associated with high free lime content [95].

The materials' setting time and mechanical properties were determined. The reference sample M-SD-2 showed the longest setting time, starting to set after about 10 h and finally setting after about 24 h. Increasing the processing temperature allows for the material to set faster. For the M-300-2 sample, the start of the setting was recorded at 5.5 hours, and the end of the setting was recorded at about 11 hours. Increasing the temperature to 450 °C (M-450-2) resulted in a significant decrease in setting time, with setting starting at just over one hour and ending at three hours. Further increasing the processing temperature to 600 °C (M-600-2), the setting time shifted by 40 minutes compared to the M-450-2 – the setting start was around 1 hour and 45 minutes and the end around 3 hours and 45 minutes. The setting start for M-750-2 and M-900-2 samples was around 5 hours, ending at 8 hours. The M-1050-2 showed high setting times as they barely held together after 24 hours. The M-1200-2 samples started to set after one hour and were fully set after just over two hours. This is explained by the amount of free lime in the material, which, when added to water, causes the lime to undergo a slaking reaction and set.

The samples' compressive strength shows (Fig. 6.4) that heating the raw materials has affected them. Treatment at different temperatures initiates different mineral and chemical changes in the material; in the case of wood additives, it is heating at 450 °C, where the wood particles burn to form charcoal, which can be considered a pozzolanic additive. For cement in M-SD-2, heating means dehydration of the hydrates formed, resulting in dehydration from the hydrate crystals and allowing the compounds to reset with water and form new hydration products. Figure 6.14 shows the compressive strength data obtained for the samples.

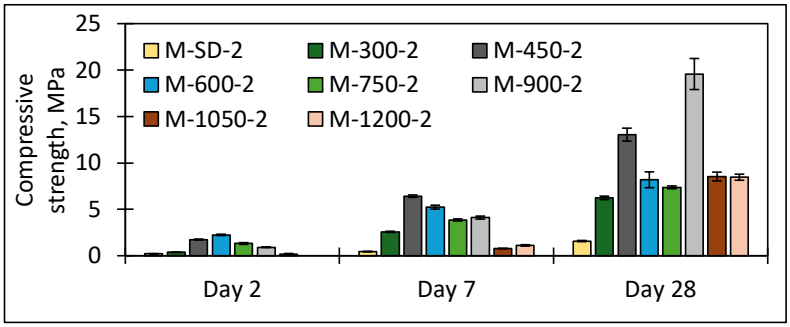

Fig. 6.4. Summary of compressive strengths for the samples.

The compressive strength of the samples also increased as they aged, which is consistent with the theory of cement hydration, meaning that hydration was successful for these samples. In the results of day 2, it can be observed that the M-600-2 shows the highest compressive strength, reaching 2.2 MPa. As the samples aged, on day 7, the M-450-2 showed the highest compressive strength, reaching 6.4 MPa, while the M-600-2 and M-900-2 also showed elevated results, reaching 5.2 MPa and 4.1 MPa. As the samples aged to day 28, the compressive strength of all samples increased. For the M-1050-2 and M-1200-2 between day 7 and day 28, the compressive strength increased rapidly from 0.8 MPa to 8.5 MPa and from 1.1 MPa to 8.5 MPa, respectively. The M-450-2 and M-900-2 showed the highest compressive strengths, reaching 13.0 MPa and 19.6 MPa on day 28, respectively.

6.2. Chapter Summary

The results strongly indicate that thermal treatment is a viable method for reactivating sanding dust (SD) as a binder. The study shows the complex interplay between thermal processing and the resulting physical, chemical, and mineralogical transformations in SD, providing critical insights for tailoring this waste material's properties to approach those of virgin cement.

Thermal gravimetric (TG) analysis across the 300–900 °C range reveals intricate decomposition patterns characteristic of both lignocellulosic and cementitious materials. The analysis highlights distinct mass loss (M-SD-2 loses 30 % of mass) stages and thermal events corresponding to specific chemical and physical changes, including initial dehydration till 200 °C, thermal degradation of wood components at around 350 °C, dihydroxylation of $Ca(OH)_2$ at 450 °C, and decarbonisation of calcium carbonate starting at 650 °C. Heat treatment influences these thermal events, reducing mass and mineralogically changing the composition of the SD.

XRF data demonstrates significant shifts in SD oxide composition with heating from 0 °C to 1200 °C. A key observation is the increase in CaO content (0 % to 14 %) and the decrease in CO_2 content (25 % to 3 %), which are directly related to the decomposition of calcium-containing compounds. Oxide changes strongly suggest the transformation of hydrated cement phases and the development of compounds more akin to cement clinker.

XRD analysis further details the mineralogical transformations during heating. At room temperature, calcite is the predominant phase at 33.3 %. As temperature increases, decomposition reactions and phase transformations occur, including the decomposition of portlandite and calcite, as described previously. Transformations within cement clinker phases are also observed. These mineralogical changes directly impact the material's potential for reuse as a binder.

The study reveals that the processing temperature significantly influences setting time and compressive strength. Higher processing temperatures generally lead to faster setting times. Furthermore, thermal treatment demonstrably affects compressive strength development in the reactivated SD, achieving 13.0 MPa and 19.6 MPa for M-450-2 and M-900-2, respectively.

7. CHARACTERISATION AND PERFORMANCE OF BIOCOMPOSITES WITH REACTIVATED BINDERS

7.1. Biocomposites with Mechanically Activated Binder

Mix Design and Sample Preparation

The binder used in this experiment is 20-minute vibration-milled, sieved sanding dust (V-20 min), and the filler is Production Line Waste (PLW), described in Section 4.1. Three compositions of bio-based building materials were made with varying binder content. The mixture design is compiled in Table 7.1.

Table 7.1

Mix Design of the Developed Bio-Based Building Materials, Mass Parts

Sample	Binder		PLW (Filler)	
	V-20 min	Water	Dry	Water for wetting*
P1	10.0	7.0	10.0	1.0
P2	5.0	3.5		
P3	3.0	2.1		

* The filler was moistened before mixing so that the filler did not absorb the water intended for the binder.

A flowchart of the sample production process is shown in Fig. 7.1. One mass part of the water was used to wet the filler material for easier incorporation of the binder, which is added after three minutes of filler and water mixing. Based on the mix design, 10, 5, and 3 mass parts of the binder were gradually added to the wet filler material and mixed, resulting in a homogeneous coating of the fibres. Afterwards, the water necessary for the binder was added to the mix. For each composition, a W/B ratio of 0.7 was used. Then, the mixture was remixed to form a homogenous composition and formed in oiled moulds of dimensions 35 cm × 35 cm × 10 cm.

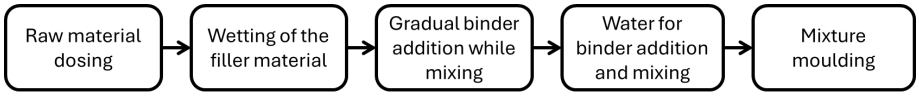

Fig. 7.1. Flowchart for biocomposite production.

Samples were demoulded after seven days, wrapped with plastic film, and cured for 21 days to ensure a minimal humidity loss for the rest of the curing process. After the curing process of 28 days, the plastic film was removed, and the samples were dried in a curing chamber at 45 °C till constant mass.

Results and Discussion

The material density of the samples ranges from 430 kg/m^3 to 613 kg/m^3. Sample P3 exhibited the lowest density (430 kg/m^3), while sample P1 had the highest density (613 kg/m^3). This variation stems

from the different binder content used during sample preparation, as documented in Table 7.1. The density values provide crucial guidance for material selection in applications where weight is critical, such as in lightweight construction elements or thermal insulation systems.

The thermal conductivity of the samples ranges from 0.083 W/(m·K) to 0.117 W/(m·K). This parameter determines the rate at which heat flows through the material, and it is an important consideration when designing thermal insulation materials. The dependence of thermal conductivity on material density is visualised in Fig. 7.2. A correlation between material density and thermal conductivity can be seen in a study by Sahmenko [96], where hempcrete samples were tested, differentiating the material density and thermal conductivity. It was found that even with different binders used, comparing that study to this study's developed materials, a conclusion can be drawn that these materials have lower thermal conductivity with the same material density. However, compressive strength is lower, as the binder is not strong.

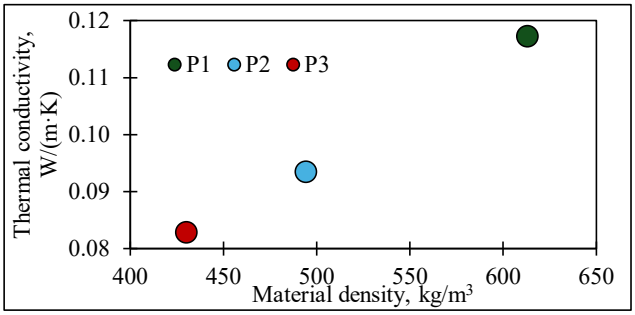

Fig. 7.2. Thermal conductivity dependence on material density.

Based on the flexural and compressive strength values provided in Table 7.2, it can be concluded that the bio-based building material exhibits moderate to low strength characteristics. The flexural strength values range from 0.06 MPa to 0.24 MPa, indicating that the material is weak in resisting bending forces. The compressive strength values are also moderate, ranging from 0.06 MPa to 0.47 MPa, depending on the forming direction.

Table 7.2

Mechanical Properties of the Developed Bio-Based Building Materials

Sample	Flexural strength, MPa	Compressive strength based on the forming direction, MPa	
		Parallel	Perpendicular
P1	0.24	0.47	0.33
P2	0.11	0.26	0.09
P3	0.06	0.18	0.06

Comparing the three developed bio-based building material prototypes, the highest values in both directions of compressive strength and flexural strength are for sample P1, reaching 0.24 MPa of flexural strength and 0.47 MPa and 0.33 MPa in parallel and perpendicular compressive strength, respectively. The lowest values were found for sample P3, which confirms that the lowest amount of binder used would result in the lowest flexural and compressive strength. P3 showed 0.06 MPa of

flexural strength, 0.18 MPa and 0.06 MPa of compressive strength in parallel and perpendicular directions. The P2 sample reached a flexural strength of 0.11 MPa and a compressive strength of 0.26 MPa in parallel and 0.09 MPa in perpendicular forming direction. The developed biocomposites had good thermal properties compared to other bio-based building materials. Biocomposites showed promise for use in envelope systems as the middle layer, filling the role of thermal insulation materials.

7.2. Biocomposites with Thermally Treated Sanding Dust

7.2.1. Biocomposites with Sanding Dust Treated at 450 °C

Mix Design and Sample Preparation

Sanding dust (SD) heat-treated at 450 °C was used as a binder (M-450-2). Production line waste (PLW) described in Section 4.1 was used as filler. Three different bio-based building material compositions were created, each with a different amount of binder. In Table 7.3, the mixture design is compiled.

Table 7.3

Mix Design of the Biocomposites Made with SD Heat-Treated at 450 °C, Mass Parts

Sample	Binder		PLW (Filler)	
	M-450-2	Water	Dry	Water for wetting*
H12	1.00	0.60	2.00	0.60
H13	0.67	0.40		
H14	0.50	0.30		

* The filler was moistened before mixing so that the filler did not absorb the water intended for the binder.

Sample preparation was done according to the flowchart in Fig. 7.1. When the sample was created, a plate was placed on top to ensure pressure and a smoother surface structure. To improve the bonding between the binder and the wood fibres, an initial pressure of 571 Pa was applied to the samples. After applying initial pressure for 60 seconds, a weight was applied to the samples to maintain a secondary pressurisation of 65 Pa as they cured. After seven days, the samples were demoulded and covered in plastic film to ensure that there was as little loss of humidity as possible, and they were cured for 21 days in room conditions (22 ± 2 °C, RH < 50 %).

Results

Thermal conductivity and mechanical properties of the developed biocomposites were evaluated. Mechanical properties include flexural and compressive strength. The samples were dried before testing for thermal conductivity. The curing chamber was set to 45 °C, and the drying process was till the mass did not change (around one week).

Material density and thermal conductivity have been compiled in Fig. 7.3. This figure reveals a positive correlation between material density and thermal conductivity in biocomposite materials with varying binder-to-filler ratios. Both properties show a clear upward trend as the ratio changes from

1 : 4 (H14) to 1 : 2 (H12). The H14 sample, with the highest filler content, shows the lowest values with approximately 370 kg/m³ material density and 0.068 W/(m·K) thermal conductivity. H13 (1 : 3 ratio), both properties increase to about 390 kg/m³ and 0.071 W/(m·K), respectively. The H12 sample, with the lowest filler content (1 : 2 ratio), exhibits the highest values at roughly 415 kg/m³ and 0.075 W/(m·K).

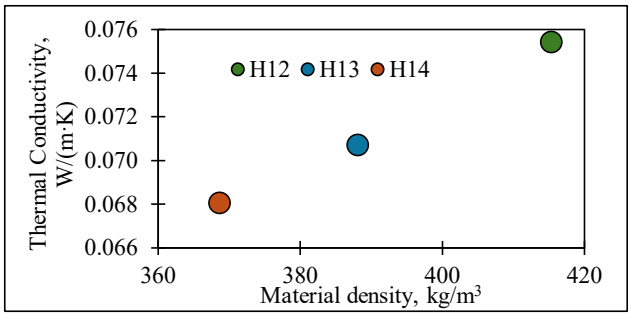

Fig. 7.3. Thermal conductivity dependence on the material density of the biocomposite samples.

This trend suggests that decreasing the filler content (or increasing the relative binder content) leads to denser materials with higher thermal conductivity [97]. This relationship is attributed to the binder potentially creating a more continuous matrix with fewer void spaces, resulting in better heat transfer pathways through the material [98]. However, it is worth noting that this is a relatively linear relationship, indicating a consistent impact of the binder-to-filler ratio on the biocomposites' physical and thermal properties [99]. This understanding could be valuable for tailoring the material properties for specific applications where either thermal insulation or conductivity is desired.

Compressive and flexural strength analysis of samples H12, H13, and H14 (Fig. 7.4.) shows variations in mechanical properties. H12 has forming direction compressive strengths of 175 ± 10 kPa (10 % deformation) and 184 ± 14 kPa (20 % deformation) and flexural strength of 100 ± 28 kPa; perpendicular strengths are lower (97 ± 13 kPa and 87 ± 42 kPa, respectively). H13 exhibits lower compressive strengths (75 ± 10 kPa and 119 ± 15 kPa in the forming direction; 27 ± 2 kPa perpendicular) and flexural strengths (31 ± 1 kPa and 64 ± 21 kPa). H14's compressive strength is higher perpendicular to the forming direction at 10 % deformation (61 ± 7 kPa vs. 26 ± 8 kPa), but this reverses at 20 % deformation (62 ± 5 kPa). H14's flexural strength is 38 ± 8 kPa. Testing direction influences the samples' mechanical properties. For better data visualisation, see Figure 7.9. has been compiled with all the mechanical properties.

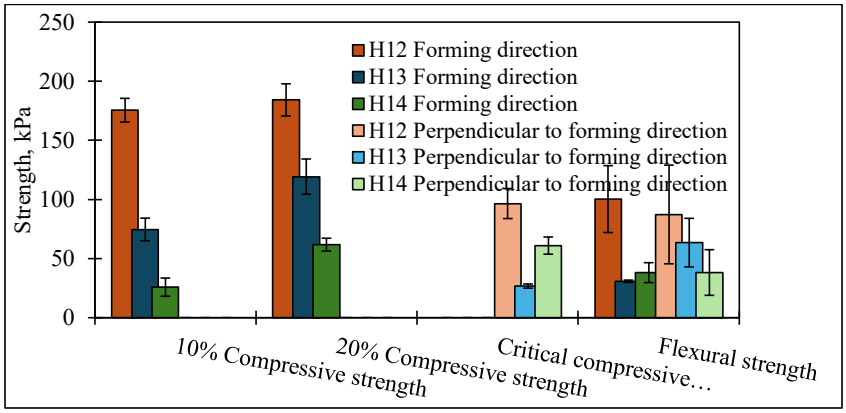

Fig. 7.4. Mechanical property compilation.

7.2.2. Biocomposites with Sanding Dust Treated at 600 °C

Mix Design and Sample Preparation

Sanding dust (SD) heat-treated at 600 °C was used as a binder (M-600-2). The properties of the binder have been characterised in Section 6.1. Production line waste (PLW) and hemp shives were bio-based aggregates. Additionally, to PLW, hemp shives were used to see how low the thermal conductivity coefficient can get, although hypothesising the result in low compressive strength. Mix designs of the biocomposites made with SD heated at 600 °C are compiled in Table 7.4.

Table 7.4

Mix Designs of the Biocomposites Made with SD Heated at 600 °C, Mass Parts

Sample	Binder		Filler		
			Dry		
	M-600-2	Water	PLW	Hemp Shives	Water for wetting*
PLW12	1.00	0.60	2.00		1.00
Hemp12				2.00	2.40
Mix12			1.00	1.00	1.80
PLW21	2.00	1.20	2.00		0.50
Hemp21				2.00	1.20
Mix21			1.00	1.00	0.85

* The filler was moistened before mixing so that the filler did not absorb the water intended for the binder.

More water was used to wet hemp shives because they absorb more than PLW. The amount of water added to the binder was the same for all samples at 0.6 mass parts of the binder. This ratio was chosen based on the results of Chapter 6. A flowchart of the sample production process is shown in Fig. 7.1. After the mixture was moulded in the forms, the surface was smoothed with a plate to obtain better surface characteristics. The samples with the plate and the load were left to cure for the first seven days until the samples were demoulded and wrapped in plastic film to ensure humidity in the samples. The

biocomposites were cured for 14 days. The samples were dried at 45 °C until a constant sample mass was obtained. For the characterisation of the material, only dry samples were used.

Results

Six different sample compositions were produced: three samples had a binder-to-filler weight ratio of 1 : 2, while the other three samples had a binder-to-filler weight ratio of 2 : 1. The main physical and mechanical properties of the material, including structure, material density, thermal conductivity, and compressive and flexural strength, were determined in experimental studies.

A clear positive correlation exists between material density and thermal conductivity across all samples (Fig. 7.5). The PLW21 sample stands out with notably higher values in both properties (782 kg/m³ material density and 0.139 W/(m·K) thermal conductivity), suggesting that production line waste at a 2 : 1 ratio creates a denser, more thermally conductive material. In contrast, Hemp12 shows the lowest values (171 kg/m³ and 0.052 W/(m·K)), indicating that hemp shives at a 1 : 2 ratio produce a lighter, more insulating material.

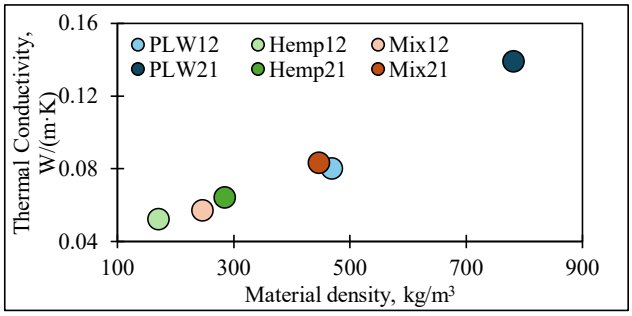

Fig. 7.5. Thermal conductivity dependence of the material density of the PLW, Hemp and Mix samples.

Foreseeably, the mix samples (Mix12 and Mix21) cluster together in the middle range (around 247–447 kg/m³ and 0.057–0.083 W/(m·K)), suggesting that combining both fillers or using PLW at a lower ratio leads to intermediate properties. Hemp21 shows slightly higher values than Hemp12 but remains relatively lightweight compared to PLW samples, demonstrating how hemp shives consistently contribute to lighter composites regardless of ratio. This variation in properties based on filler type and ratio provides flexibility in tailoring the biocomposites for different applications, from insulation (hemp-rich compositions) to structural applications (PLW-rich compositions).

Figure 7.6 shows the flexural strength results of the biocomposites produced. The biocomposites exhibit flexural strengths up to 288 kPa depending on the composition.

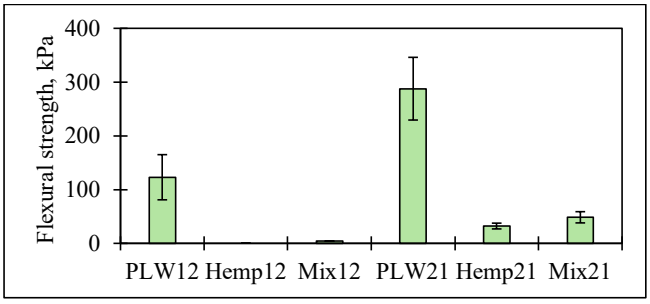

Fig. 7.6. Flexural strength of the samples.

The results show that the presence of hemp shives in the material significantly reduces the flexural strength of the sample. This is due to the relatively lower contact zone and high water uptake in hemp shive biocomposites, which release bioactive substances, reducing the strength.

Compressive strength was tested at 10 % strain for all samples and at the failure load for the PLW21 sample, as this was the only sample where the load/deformation curves showed a pronounced failure of the material. Figure 7.7 shows the compressive strength results of the biocomposites produced. The compressive strength of the biocomposites produced parallel to the forming direction varies from 0.02 MPa to 1.65 MPa, depending on the filler used and the binder/filler ratio. For the Mix12 samples, performing a compressive strength test was impossible due to the material being brittle.

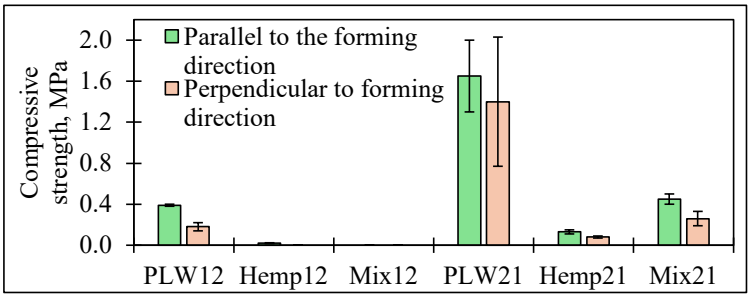

Fig. 7.7. Compressive strength of the biocomposites at 10 % strain.

Compared to commercially available wood-wool cement panels, the PLW12 sample produced is similar in properties to commercial wood-wool cement panels with a compressive strength parallel to the direction of forming of 0.3 MPa. It should be noted that commercial wood-wool cement panels are produced more homogeneously, so the experimental results could be improved by modifying the fabrication technology. The PLW21 sample shows more than twice the compressive strength of PLW12, although the material density of these biocomposites differs by less than a factor of two.

The compressive strength of the samples is perpendicular to the direction of forming, and in all cases, it is approximately twice as low as parallel to the direction of forming. This indicates that all the biocomposites produced are anisotropic and that their mechanical properties vary significantly depending on the orientation of the filler in the material and the operating direction.

Given the study's objective to investigate the use of wood-wool cement panel production wastes, the two biocomposites produced (PLW12 and PLW21) were compared with commercially available acoustic wood-wool cement panel sheets produced by Cewood Ltd. The comparison is shown in Table 7.5.

Table 7.5

Comparison of the Properties of the Manufactured Biocomposites and the Wood-Wool Cement Panels Produced by Cewood Ltd.

Property	Cewood acoustic panel	PLW12	PLW21
Width of the fibre, mm	1.5	1.5	1.5
Thickness, mm	25	40	31
Material density of material, kg/m^3	420	470	780
Thermal conductivity (λD), W/(m·K)	0.066	0.080	0.139
Flexural strength (EN 12089), kPa	≥ 1300	≥ 75	≥ 220
Compressive strength (EN 826), kPa	≥ 300	≥ 380	≥ 1500

As shown in the table, the biocomposites produced in the study have lower flexural strength (≥ 220 kPa PLW21 and ≥ 75 kPa PLW12) and higher compressive strength (≥ 1500 kPa PLW21 and ≥ 380 kPa PLW12) than commercially available materials. Although commercial wood-wool cement panel products are made with fresh cement and longer wood shavings, the results of this study can be considered satisfactory. PLW21 is unsuitable for visual aspects, while PLW12 is comparable to Cewood panels.

7.3. Biocomposites with CEM II/A-LL 42.5 N

Mix Design and Sample Preparation

CEM II/A-LL 42.5 N was used as the binder to compare the biocomposites' properties with the properties of biocomposites made with the developed binders. By using a commercially available binder, a comparison of the effectiveness of the developed binders can be made.

Production line waste (PLW) was examined as a filler to produce biocomposites. The effect of the binder-to-filler ratio was examined and evaluated. The biocomposites were prepared with different CEM II/A-LL 42.5 N to PLW ratios (Table 7.9). The CEM II/A-LL 42.5 N to PLW ratio was 1 : 2, 1 : 3, and 1 : 4. The water-to-filler (W/F) ratio was increased with the increase of PLW content in the mixture composition. The 1 : 2 mixture had a W/F ratio of 0.7. In mixture 1 : 3, it increased to 1.3; for 1 : 4, the W/F increased to 1.6. In previous research, water could reach and be above a 1 : 1 ratio to filler content [100–102].

A partial PLW substitution with the hemp shives (HS) was evaluated to reduce the material density of biocomposites. Previous research showed that adding HS allows the obtaining of biocomposites with a material density of 200 kg/m^3 to 400 kg/m^3 [103]. The replacement of 25 %, 50 % and 75 % by the weight of PLW with HS was assumed (Table 7.6). The CEM II/A-LL 42.5 N to filler ratio remained 1 : 2 by weight. The bulk material density of HS is significantly lower than that of PLW (100 kg/m^3 for HS compared to 300 kg/m^3 for PLW).

Table 7.6

Mix Designs of the Biocomposites Made with CEM II/A-LL 42.5 N, Mass Parts

Sample	Binder		Filler		
	CEM II/A-LL 42.5 N	Water	Dry		Water for wetting*
			PLW	Hemp Shives	
I	1.0	0.4	2.0		0.7
II			3.0		1.3
III			4.0		1.6
H25			1.5	0.5	1.4
H50			1.0	1.0	1.6
H75			0.5	1.5	2.0

* The filler was moistened before mixing so that the filler did not absorb the water intended for the binder.

All dry components were weighed, but before mixing (Fig. 7.8 a)), fillers were mixed with water to wet the surface for 2 min (Fig. 7.8 b)). A single-shaft electrical mixer, RubiMix, was used for mixing. Then, CEM II/A-LL 42.5 N was added, and the mixture was homogenised for 2 min (Fig. 7.8 c)). Then, the mixture was cast in prepared moulds (Fig. 7.8 d)). The samples with a surface area of 35 cm × 35 cm and a thickness of 5 cm to 10 cm were prepared for further testing.

Fig. 7.8. Mixing procedure of biocomposites: a) PLW filler; b) filler wetting; c) binder incorporation in the mixture; d) casting of the biocomposite.

Results and Discussion

Figure 7.9 shows a clear transition in material behaviour. Samples I, II, and III (with PLW filler) show higher material densities (391–474 kg/m³) and thermal conductivity values (0.070–0.082 W/(m·K)). As hemp shive percentage increases from 0 % to 75 %, material density and thermal conductivity decrease systematically, with H75 showing the lowest values of 197 kg/m³ and 0.054 W/(m·K). This trend can be attributed to hemp's inherent lightweight nature and cellular structure, as documented by Arnaud and Gourlay [104].

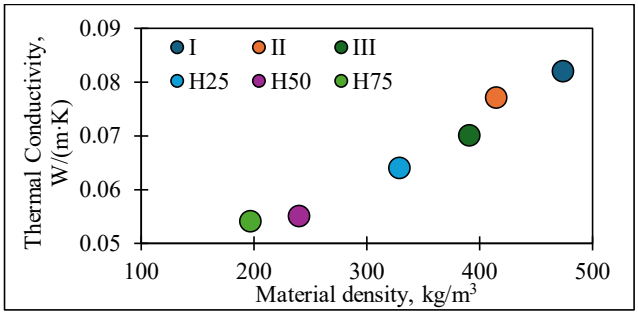

Fig. 7.9. Thermal conductivity dependence on material density.

The compilation of data on mechanical strength is given in Fig. 7.10. H50 and H75 were too brittle to test, and thus, we concluded that those samples were not feasible for the objectives of this Thesis. The highest amount of CEM II/A-LL 42.5 N in the biocomposite Sample I shows a flexural strength of 0.31 MPa and compressive strength of 0.56 MPa at 20 % deformation. The reduction of the CEM II/A-LL 42.5 N (Sample II) led to a decrease in flexural strength of 0.12 MPa and compressive strength of 0.31 MPa at 20 % deformation. Flexural strength of Sample III achieved 0.06 MPa and a compressive strength of 0.21 MPa at 20 % deformation. However, the lowest strength was for a mixture with HS. It was possible to test only H25, and the flexural strength was 0.02 MPa, and the compressive strength achieved 0.20 MPa at 20 % deformation.

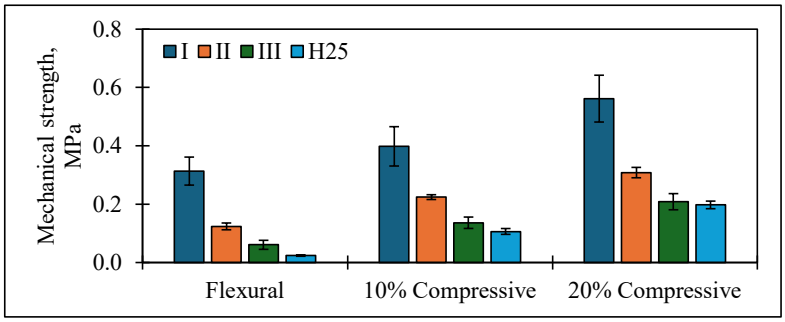

Fig. 7.10. Mechanical strength compilation of biocomposites.

7.4. Demonstration of Biocomposites

The workability and feasibility of the biocomposite made with a mechanically activated binder were practically approbated in a semi-industrial setting. An experimental stand (Fig. 7.11) was built using two compositions of the developed biocomposites. The binder used was vibration-milled SD that was milled for 20 minutes. A vibration mill was used because of its capacity to mill larger amounts of material than a planetary mill. The filler was PLW (Fig. 4.1), collected from the WWCP manufacturing plant a few days prior to building. The construction of the experimental stand took two days.

Fig. 7.11. Timber frame of the experimental stand.

Two walls were filled with the designed material. Both walls had slight variations in composition for the variety of results. On the first day, measurements of the materials were taken to increase work effectiveness later. The density of the dry wool was determined using a bucket of a specific volume into which the wool was placed and weighed, and the density was calculated. The bulk density was about 70 kg/m^3, while when the material was compressed (simulating a fill in a partition), the density was about 200 kg/m^3, which varied when the wool was wet or dry. In the case of wet wool, the density can reach 270 kg/m^3. Both the binder and filler were weighed before each mixing.

The inner and outer layers of the timber frame consisted of defective WWCP, which were then filled in the middle with the developed biocomposite.

The filler was poured into a drum mixer, and water was added to moisten the wood-wool in the ratio of 0.15 of the mass of the filler. Then, the binder was added in the ratio of 0.25–0.30 of the filler mass and mixed. When the binder had been dispersed, more water was added in a ratio of 0.60 of the amount of the binder's mass. Everything was mixed for two minutes and, with slight packing, was filled into the wall.

With the construction of this experimental stand, smaller laboratory-scale samples with dimensions 600 mm x 600 mm x 180 mm were made (Fig. 7.12). The laboratory samples were made from two defective WWCPs fastened to each side of a wooden frame, with the top part also being a WCP. The middle layer of the panel consisted of the developed material. The panels were tested for their density and thermal conductivity. The composition of laboratory samples was the same as the experimental stand and was close to the P3 sample in Section 7.1. The density for the whole panel was 323 kg/m^3 with a thermal conductivity of 0.0709 W/(m·K). The middle layer was then taken out of the form and tested separately. It achieved a 245 kg/m^3 density with a thermal conductivity of 0.0796 W/(m·K).

Fig. 7.12. Laboratory sample of the experimental stand.

After the walls had been filled and sensors placed, the experimental stand looked as seen in Fig. 7.13. Afterwards, construction of the experimental stand continued, with a roof, doors, façade, and heating system added. As of now, the house still stands and is in use.

Fig. 7.13. Experimental stand completed with multilayer panels.

7.5. Chapter Summary

This research explored biocomposites with various binders for sustainable construction. Mechanically activated sanding dust (V-20 min) showed that higher binder content increased density (613–430 kg/m³) and improved mechanical properties, achieving up to 236 kPa flexural and 469 kPa/330 kPa compressive strength (parallel/perpendicular). Conversely, lower binder content enhanced thermal insulation (down to 0.083 W/(m·K)), with an inverse relationship between strength and thermal performance observed across binders.

Biocomposites with SD treated at 450 °C (369–415 kg/m³) showed similar density-thermal conductivity correlation (0.068–0.075 W/(m·K)). Denser samples had higher mechanical strength, and all samples displayed anisotropic behaviour. Composites with SD treated at 600 °C showed potential, but with binder adhesion issues affecting hemp shive mixes. Hemp improved thermal performance (down to 0.052 W/(m·K)) at the cost of mechanical strength. Portland cement composites using recycled wood-wool achieved 391–511 kg/m³ density. Hemp addition reduced density (down to 197 kg/m³) and improved thermal performance (0.054 W/(m·K)), yielding self-bearing thermal insulation.

Across binders, lower density improved thermal properties (hemp mixes reaching 0.052–0.054 W/(m·K)), while higher density increased mechanical strength; anisotropic behaviour was common. Mechanically activated SD offers a balance of properties. Hemp shive addition is suited for a lower thermal insulation coefficient. Recycled wood-wool cement composites show circular economy potential. These biocomposites are viable alternatives for applications needing balanced strength and insulation, such as non-load-bearing walls and insulation. An experimental stand validated the workability of mechanically activated binder composites. Future work will optimise material properties, assess long-term performance and environmental impact, and scale production.

8. LIFE CYCLE ASSESSMENT OF THE DEVELOPED BUILDING MATERIALS

Developed biocomposites with the proposed compressive strength of 0.05 MPa embedded in an envelope system were compared with commercially used envelope systems. Commercial systems included Autoclaved Aerated Concrete (AAC), Expanded Clay Cement Block (ECCB) and Ceramic Building Block (CBB) as load-bearing materials and expanded polystyrene (EPS), Stone Wool (SW) 15 and 80 as thermal insulation materials. All compared envelope systems provide a U-value of 0.18 W/m^2·K. The system used with the developed biocomposites has a lot of thermal inertia, so a comparison was made with similar materials.

The LCA data presented in Fig. 8.1 demonstrates the significant environmental advantage of the newly developed biocomposites compared to conventional building envelope systems. The four biocomposite variants (Vibro(0.05), 450(0.05), 600(0.05), and CEM(0.05)) exhibit remarkably lower carbon footprints, ranging from 6.9 kg CO_2 eq. to 17.0 kg CO_2 eq., with Vibro(0.05) showing the lowest environmental impact at just 6.9 kg CO_2 eq.

In contrast, conventional building systems display higher carbon emissions. The AAC-EPS system produces 67.8 kg CO_2 eq., while AAC-SW 80 and ECCB-EPS generate 72.1 kg CO_2 eq. and 70.8 kg CO_2 eq., respectively. The highest emissions are associated with ECCB-SW 15 at 86.3 kg CO_2 eq., followed by CBB-SW 80 (83.0 kg CO_2 eq.) and CBB-EPS (79.7 kg CO_2 eq.).

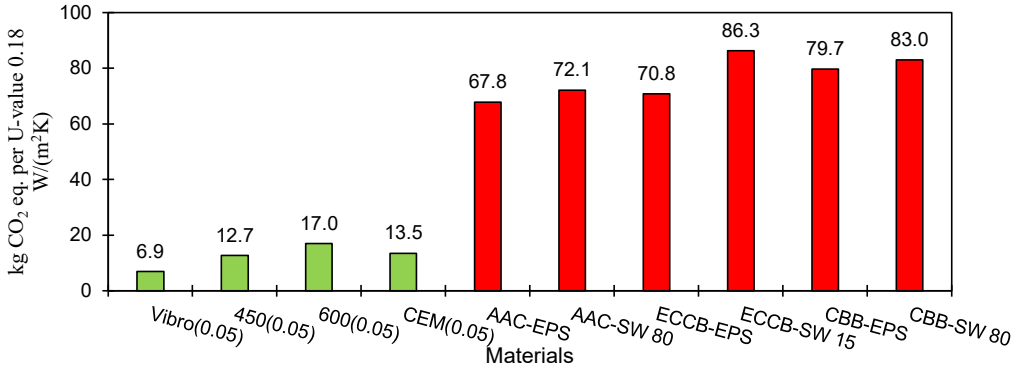

Fig. 8.1. Emission comparison with conventional wall assembly systems.

This comparison reveals that the biocomposites developed from wood-wool cement panel manufacturing and production line waste achieve carbon emissions reductions of approximately 75–90 % compared to conventional systems. Even the highest-emitting biocomposite system (600(0.05) at 17.0 kg CO_2 eq.) still produces only about 25 % of the carbon emissions of the most environmentally friendly conventional system (ACC-EPS at 67.8 kg CO_2 eq.).

These biocomposites represent a promising advancement for sustainable construction materials. Their ability to achieve the required thermal performance (U-value of 0.18 W/m²K) while dramatically reducing embodied carbon makes them particularly valuable for low-carbon building initiatives. The circular economy approach – repurposing manufacturing waste streams as binder and filler – aligns perfectly with growing industry demands for waste reduction and resource efficiency.

CONCLUSIONS

This research explores recycling wood-wool cement panel (WWCP) waste through advanced material reactivation and biocomposite development, transforming industrial waste into potential construction materials via mechanical, thermal, and chemical treatments.

Three milling techniques were investigated:

- Collision milling produced a binder with up to 5 MPa compressive strength in 180 days (1.7 MPa in 28 days).
- Planetary ball milling improved sanding dust's cementitious properties; high humidity and water curing yielded compressive strengths of 1.9 MPa and 2.2 MPa, respectively, with the optimal water-to-binder ratio being 0.6–0.8. Milling for 15 minutes quadrupled compressive strength to 6.50 MPa in 28 days.
- Vibration milling's optimal processing time was 15 minutes for workability, while 20 minutes achieved 1.6 MPa compressive strength in 28 days.

Two heat treatment methods were analysed:

- Muffle furnace treatment showed optimal temperatures at 450 °C and 900 °C, achieving compressive strengths of 13.0 MPa and 19.6 MPa on the 28th day.
- Rotary kiln treatment at 450 °C and 900 °C improved strength (13.8 MPa and 18.6 MPa at 180 days, ~10 MPa on day 28 for both compositions) compared to raw material (2.5 MPa on day 180 and 1.0 MPa on day 28).

Mechanical activation achieved moderate strengths (5–15 MPa), while thermal treatments, especially muffle furnace treatment at 900°C, yielded the highest compressive strength (19.6 MPa).

Biocomposites showed an inverse relationship between thermal and mechanical properties: higher binder content (P1) achieved better mechanical properties (236 kPa flexural, 469/330 kPa compression) at 613 kg/m³. In comparison, lower binder content (P3) provided better insulation (0.083 W/(m·K)) at 430 kg/m³. Hemp shives substitution improved thermal performance, reducing thermal conductivity to 0.054 W/(m·K).

This research demonstrates the feasibility of transforming WWCP waste into valuable materials, balancing thermal insulation and mechanical strength, and promoting circular economy principles.

REFERENCES

1. Moschen-Schimek, J.; Kasper, T.; Huber-Humer, M. Critical Review of the Recovery Rates of Construction and Demolition Waste in the European Union – An Analysis of Influencing Factors in Selected EU Countries. *Waste Management* **2023**, *167*, 150–164, doi:10.1016/J.WASMAN.2023.05.020.
2. APlanet European Green Deal: Objectives and Initiatives for a Sustainable Future Available online: https://aplanet.org/resources/european-green-deal-objectives-and-initiatives-for-a-sustainable-future/ (accessed on 7 January 2025).
3. Rueda Raya, S.; Tolentino-Zondervan, F.; van Winden, W.; van Hemert, P. *CURE+ Baseline Study: City of Riga, Latvia*;
4. Klimata un enerģētikas ministrija *Latvijas Nacionālais Enerģētikas un Klimata Plāns 2021.-2030. gadam*; Riga, 2024;
5. European Commision A New Circular Economy Action Plan Available online: https://eur-lex.europa.eu/legal-content/EN/TXT/?qid=1583933814386&uri=COM:2020:98:FIN#footnote33 (accessed on 2 January 2025).
6. Schneider, M.; Romer, M.; Tschudin, M.; Bolio, H. Sustainable Cement Production—Present and Future. *Cem Concr Res* **2011**, *41*, 642–650, doi:10.1016/J.CEMCONRES.2011.03.019.
7. Wu, M.; Zhang, Y.; Ji, Y.; Liu, G.; Liu, C.; She, W.; Sun, W. Reducing Environmental Impacts and Carbon Emissions: Study of Effects of Superfine Cement Particles on Blended Cement Containing High Volume Mineral Admixtures. *J Clean Prod* **2018**, *196*, 358–369, doi:10.1016/J.JCLEPRO.2018.06.079.
8. Argalis, P.P.; Sinka, M.; Bajare, D. A Preliminary Study of Mechanical Treatments' Effect on the Reactivation of Hydrated Cement Paste. *J Phys Conf Ser* **2023**, *2423*, 012008, doi:10.1088/1742-6596/2423/1/012008.
9. Gholizadeh-Vayghan, A.; Meza Hernandez, G.; Kingne, F.K.; Gu, J.; Dilissen, N.; El Kadi, M.; Tysmans, T.; Vleugels, J.; Rahier, H.; Snellings, R. Thermal Reactivation of Hydrated Cement Paste: Properties and Impact on Cement Hydration. *Materials 2024, Vol. 17, Page 2659* **2024**, *17*, 2659, doi:10.3390/MA17112659.
10. Yang, H.; Che, Y.; Leng, F. Calcium Leaching Behavior of Cementitious Materials in Hydrochloric Acid Solution. *Scientific Reports 2018 8:1* **2018**, *8*, 1–9, doi:10.1038/s41598-018-27255-x.
11. Cordoba, G.; Paulo, C.I.; Irassar, E.F. Towards an Eco-Efficient Ready Mix-Concrete Industry: Advances and Opportunities. A Study of the Metropolitan Region of Buenos Aires. *Journal of Building Engineering* **2023**, *63*, 105449, doi:10.1016/J.JOBE.2022.105449.
12. Joseph, H.S.; Pachiappan, T.; Avudaiappan, S.; Maureira-Carsalade, N.; Roco-Videla, Á.; Guindos, P.; Parra, P.F. A Comprehensive Review on Recycling of Construction Demolition Waste in Concrete. *Sustainability 2023, Vol. 15, Page 4932* **2023**, *15*, 4932, doi:10.3390/SU15064932.
13. Puskás, A.; Corbu, O.; Szilágyi, H.; Moga, L.M. Construction Waste Disposal Practices: The Recycling and Recovery of Waste. *WIT Transactions on Ecology and the Environment* **2014**, *191*, 1313–1321, doi:10.2495/SC141102.

14. Ahmad, Z.; Wee, L. siong; Fauzi, M.A. Mechanical Properties of Wood-Wool Cement Composite Board Manufactured Using Selected Malaysian Fast Grown Timber Species. *ASM Science Journal* **2011**, *5*, 27–35.
15. Mordor Intelligence *Cement Board Market - Share & Size*; 2024;
16. Gibbs, M.J.; Soyka, P.; Conneely, D. CO2 EMISSIONS FROM CEMENT PRODUCTION. *Good Practice Guidance and Uncertainty Management in National Greenhouse Gas Inventories* **2001**, 175–182.
17. Wang, P.; Ryberg, M.; Yang, Y.; Feng, K.; Kara, S.; Hauschild, M.; Chen, W.-Q. Efficiency Stagnation in Global Steel Production Urges Joint Supply- and Demand-Side Mitigation Efforts. *Nat Commun* **2021**, *12*, 2066, doi:10.1038/s41467-021-22245-6.
18. Andrew, R.M. Global CO2 Emissions from Cement Production., doi:10.5281/zenodo.831454.
19. Eurostat Employment by Main Industry Available online: https://ec.europa.eu/eurostat/databrowser/view/nama_10_a10_e__custom_5685302/bookmark/table?lang=en&bookmarkId=cb2322c2-810c-4ae0-84e3-dacb1c60ca75 (accessed on 8 April 2025).
20. Official statistics of Latvia *Forests of Latvia*; Riga, 2024;
21. Central Statistical Bureau Extraction of Raw Materials for Building Materials 2023.
22. European Investment Bank Riga Water Company Modernises the Water Infrastructure in the Capital Available online: https://www.eib.org/en/stories/riga-water-infrastructure-sustainable (accessed on 2 January 2025).
23. Tamma, P.; Schaart, E.; Gurzu, A. Europe's Green Deal Plan Unveiled Available online: https://www.politico.eu/article/the-commissions-green-deal-plan-unveiled/ (accessed on 2 January 2025).
24. GRESB Establishing an Embodied Carbon Strategy in the EU Market Available online: https://www.gresb.com/nl-en/establishing-an-embodied-carbon-strategy-in-the-eu-market/ (accessed on 2 January 2025).
25. Liselotte, J. *Latvia's Climate Action Strategy*; 2024;
26. Saeima of Latvia *Būvniecības Likums*; Latvijas Vēstnesis: Riga, 2014;
27. Enterprise Agency, N. *The Circularity in Construction Sector in Latvia Opportunities and Obstacles for Dutch Entrepreneurs Commissioned by the Netherlands Enterprise Agency*;
28. Wolff, G. *Resource Efficient Use of Mixed Wastes Improving Management of Construction and Demolition Waste - Final Report*; 2017;
29. ISM waste & recycling What Is the Waste Hierarchy? Available online: https://ismwaste.co.uk/help/what-is-the-waste-hierarchy (accessed on 3 January 2025).
30. Gibbs, M.J.; Soyka, P.; Connely, D. CO 2 Emissions from Cement Production. In *Good Practice Guidance and Uncertainty Management in National Greenhouse Gas Inventories*; 2021; pp. 175–182.
31. Irish Green Building Council Level(s) - EU Sustainable Buildings Framework Available online: https://www.igbc.ie/certification/levels-eu-sustainable-buildings-framework (accessed on 7 January 2025).
32. European Environment Agency *Circular Economy Country Profile-Latvia*;
33. Myronycheva, O.; Karlsson, O.; Sehlstedt-Persson, M.; Öhman, M.; Sandberg, D. Distribution of Low-Molecular Lipophilic Extractives beneath the Surface of Air- and Kiln-Dried Scots Pine Sapwood Boards. *PLoS One* **2018**, *13*, e0204212, doi:10.1371/JOURNAL.PONE.0204212.

34. Bumanis, G.; Argalis, P.P.; Sinka, M.; Korjakins, A.; Bajare, D. The Use of Recycled Cement-Bonded Particle Board Waste in the Development of Lightweight Biocomposites. *Materials* **2024**, *17*, 5890, doi:10.3390/ma17235890.
35. Cewood CEWOOD — Wood Wool Panels Available online: https://www.cewood.com/downloads-eng (accessed on 15 January 2025).
36. Argalis, P.P.; Sinka, M.; Bajare, D. Recycling of Cement–Wood Board Production Waste into a Low-Strength Cementitious Binder. *Recycling* **2022**, *7*, 76, doi:10.3390/recycling7050076.
37. Bumanis, G.; Argalis, P.P.; Sinka, M.; Korjakins, A.; Bajare, D. The Use of Recycled Cement-Bonded Particle Board Waste in the Development of Lightweight Biocomposites. *Materials* **2024**, *17*, 5890, doi:10.3390/ma17235890.
38. Suarez-Riera, D.; Restuccia, L.; Falliano, D.; Ferro, G.A.; Tuliani, J.M.; Pavese, M.; Lavagna, L. An Overview of Methods to Enhance the Environmental Performance of Cement-Based Materials. *Infrastructures 2024, Vol. 9, Page 94* **2024**, *9*, 94, doi:10.3390/INFRASTRUCTURES9060094.
39. Kaptan, K.; Cunha, S.; Aguiar, J. A Review of the Utilization of Recycled Powder from Concrete Waste as a Cement Partial Replacement in Cement-Based Materials: Fundamental Properties and Activation Methods. *Applied Sciences 2024, Vol. 14, Page 9775* **2024**, *14*, 9775, doi:10.3390/APP14219775.
40. Seghir, N.T.; Benaimeche, O.; Krzywínski, K.; Sadowski, L. Ultrasonic Evaluation of Cement-Based Building Materials Modified Using Marble Powder Sourced from Industrial Wastes. *Buildings 2020, Vol. 10, Page 38* **2020**, *10*, 38, doi:10.3390/BUILDINGS10030038.
41. Burmeister, C.F.; Kwade, A. Process Engineering with Planetary Ball Millss. *Chem Soc Rev* **2013**, *42*, 7660–7667, doi:10.1039/c3cs35455e.
42. Tiwari, P. *SIZE REDUCTION*; Kanpur, 2023;
43. Alpha Grinding Media What Is a Ball Mill Machine? Its Types and Uses Available online: https://alphagrindingmedia.com/what-are-ball-mill-machines-and-why-do-i-use-them/ (accessed on 13 December 2024).
44. Tantawy, M.A. Effect of High Temperatures on the Microstructure of Cement Paste. *Journal of Materials Science and Chemical Engineering* **2017**, *05*, 33–48, doi:10.4236/MSCE.2017.511004.
45. Ebben, A.; Carlson, C. Top Applications for Rotary Kilns Available online: https://feeco.com/top-applications-rotary-kilns/ (accessed on 13 December 2024).
46. Choi, H.; Lim, M.; Choi, H.; Kitagaki, R.; Noguchi, T.; Choi, H.; Lim, M.; Choi, H.; Kitagaki, R.; Noguchi, T. Using Microwave Heating to Completely Recycle Concrete. *J Environ Prot (Irvine, Calif)* **2014**, *5*, 583–596, doi:10.4236/JEP.2014.57060.
47. Barbhuiya, S.; Kanavaris, F.; Das, B.B.; Idrees, M. Decarbonising Cement and Concrete Production: Strategies, Challenges and Pathways for Sustainable Development. *Journal of Building Engineering* **2024**, *86*, doi:10.1016/J.JOBE.2024.108861.
48. Dunant, C.F.; Joseph, S.; Prajapati, R.; Allwood, J.M. Electric Recycling of Portland Cement at Scale. *Nature 2024 629:8014* **2024**, *629*, 1055–1061, doi:10.1038/s41586-024-07338-8.
49. Ho, H.J.; Iizuka, A.; Shibata, E. Chemical Recycling and Use of Various Types of Concrete Waste: A Review. *J Clean Prod* **2021**, *284*, 124785, doi:10.1016/J.JCLEPRO.2020.124785.
50. Marmier, A. Decarbonisation Options for the Cement Industry.; 2000.

51. Lam, L.; Wong, Y.L.; Poon, C.S. Effect of Fly Ash and Silica Fume on Compression and Fracture Behaviors of Concrete. *Cem Concr Res* **1998**, *28*, 271–283, doi:10.1016/S0008-8846(97)00269-X.
52. EPD Norway *Environmental Product Declaration*; 2024;
53. Zorica, J.; Sinka, M.; Sahmenko, G.; Vitola, L.; Korjakins, A.; Bajare, D. Hemp Biocomposite Boards Using Improved Magnesium Oxychloride Cement. *Energies (Basel)* **2022**, *15*, doi:10.3390/EN15197320.
54. ASTM International Standard Test Method for Sieve Analysis of Fine and Coarse Aggregates. *Annual Book of ASTM Standards* 2011, 5–9.
55. Zimele, Z.; Sinka, M.; Bajare, D.; Jakovics, A. Life Cycle Assessment for Masonry Exterior Wall Assemblies Made of Traditional Building Materials. *IOP Conf Ser Mater Sci Eng* **2019**, *660*, doi:10.1088/1757-899X/660/1/012042.
56. Shi, Y.; Wang, T.; Li, H.; Wu, S. Exploring the Influence Factors of Early Hydration of Ultrafine Cement. *Materials* **2021**, *14*, 5677, doi:10.3390/MA14195677.
57. Lv, L.; Luo, S.; Šavija, B.; Zhang, H.; Li, L.; Ueda, T.; Xing, F. Effect of Particle Size Distribution on the Pre-Hydration, Hydration Kinetics, and Mechanical Properties of Calcium Sulfoaluminate Cement. *Constr Build Mater* **2023**, *398*, 132497, doi:10.1016/j.conbuildmat.2023.132497.
58. Rajczakowska, M.; Nilsson, L.; Habermehl-Cwirzen, K.; Hedlund, H.; Cwirzen, A. Does a High Amount of Unhydrated Portland Cement Ensure an Effective Autogenous Self-Healing of Mortar? *Materials 2019, Vol. 12, Page 3298* **2019**, *12*, 3298, doi:10.3390/MA12203298.
59. Gholizadeh-Vayghan, A.; Meza Hernandez, G.; Kingne, F.K.; Gu, J.; Dilissen, N.; El Kadi, M.; Tysmans, T.; Vleugels, J.; Rahier, H.; Snellings, R. Thermal Reactivation of Hydrated Cement Paste: Properties and Impact on Cement Hydration. *Materials* **2024**, *17*, 2659, doi:10.3390/ma17112659.
60. Shui, Z.; Xuan, D.; Wan, H.; Cao, B. Rehydration Reactivity of Recycled Mortar from Concrete Waste Experienced to Thermal Treatment. *Constr Build Mater* **2008**, *22*, 1723–1729, doi:10.1016/j.conbuildmat.2007.05.012.
61. Ermilova, E.; Kamalova, Z. The Influence of Complex Additives Based on Calcined Clays and Carbonate Fillers on Hydration Products Composition of Blended Cement Stone. *E3S Web of Conferences* **2021**, *274*, 04004, doi:10.1051/e3sconf/202127404004.
62. Ye, G.; Liu, X.; De Schutter, G.; Poppe, A.M.; Taerwe, L. Influence of Limestone Powder Used as Filler in SCC on Hydration and Microstructure of Cement Pastes. *Cem Concr Compos* **2007**, *29*, 94–102, doi:10.1016/j.cemconcomp.2006.09.003.
63. Poletto, M.; Zattera, A.J.; Santana, R.M.C. Thermal Decomposition of Wood: Kinetics and Degradation Mechanisms. *Bioresour Technol* **2012**, *126*, 7–12, doi:10.1016/J.BIORTECH.2012.08.133.
64. Brandt, A.M.; Marks, M. Optimization of the Material Structure and Composition of Cement Based Composites. *Cem Concr Compos* **1996**, *18*, 271–279, doi:10.1016/0958-9465(96)00018-2.
65. Scrivener, K.; Snellings, R.; Lothenbach, B. A Practical Guide to Microstructural Analysis of Cementitious Materials / Edited by Karen Scrivener, Ruben Snellings, Barbara Lothenbach. **2016**, 420–442.

66. Boualleg, S.; Bencheikh, M.; Belagraa, L.; Daoudi, A.; Chikouche, M.A. The Combined Effect of the Initial Cure and the Type of Cement on the Natural Carbonation, the Portlandite Content, and Nonevaporable Water in Blended Cement. *Advances in Materials Science and Engineering* **2017**, *2017*, doi:10.1155/2017/5634713.
67. Fraga, L.G.; Silva, J.; Teixeira, S.; Soares, D.; Ferreira, M.; Teixeira, J. Influence of Operating Conditions on the Thermal Behavior and Kinetics of Pine Wood Particles Using Thermogravimetric Analysis. *Energies (Basel)* **2020**, *13*, 2756, doi:10.3390/en13112756.
68. Mohsen, A.; Aiad, I.; El-Hossiny, F.I.; Habib, A.O. Evaluating the Mechanical Properties of Admixed Blended Cement Pastes and Estimating Its Kinetics of Hydration by Different Techniques. *Egyptian Journal of Petroleum* **2020**, *29*, 171–186, doi:10.1016/j.ejpe.2020.03.001.
69. Santos, T.A.; De Oliveira Silva, G.A.E.; Ribeiro, D.V. Mineralogical Analysis of Portland Cement Pastes Rehydrated. *Journal of Solid Waste Technology and Management* **2020**, *46*, 15–23, doi:10.5276/JSWTM/2020.15.
70. Ifguis, O.; Moutcine, A.; Laghlimi, C.; Ziat, Y.; Bouhdadi, R.; Chtaini, A.; Moubarik, A.; Mbarki, M. Biopolymer-Modified Carbon Paste Electrode for the Electrochemical Detection of Pb(II) in Water. *J Anal Methods Chem* **2022**, *2022*, doi:10.1155/2022/5348246.
71. Alonso, C.; Fernandez, L. Dehydration and Rehydration Processes of Cement Paste Exposed to High Temperature Environments. *J Mater Sci* **2004**, *39*, 3015–3024, doi:10.1023/B:JMSC.0000025827.65956.18.
72. Kim, H.S.; Kim, S.; Kim, H.J.; Yang, H.S. Thermal Properties of Bio-Flour-Filled Polyolefin Composites with Different Compatibilizing Agent Type and Content. *Thermochim Acta* **2006**, *451*, 181–188, doi:10.1016/J.TCA.2006.09.013.
73. Angelescu, N.; Stanciu, D.; Barroso de Aguiar, J.; Abdelgader, H.S.; Bratu, V. Role of Superplasticizer Additives Upon Hydration Process of Cement Pastes. *Scientific Bulletin of Valahia University - Materials and Mechanics* **2016**, *14*, 23–26, doi:10.1515/bsmm-2016-0004.
74. Santhanam, M.; Cohen, M.D.; Olek, J. Sulfate Attack Research - Whither Now? *Cem Concr Res* **2001**, *31*, 845–851, doi:10.1016/S0008-8846(01)00510-5.
75. Kucharczyk, S.; Zajac, M.; Deja, J. The Influence of Limestone and Al2O3 Content in the Slag on the Performance of the Composite Cements. *Procedia Eng* **2015**, *108*, 402–409, doi:10.1016/j.proeng.2015.06.164.
76. Habte, L.; Shiferaw, N.; Mulatu, D.; Thenepalli, T.; Chilakala, R.; Whan Ahn, J. Synthesis of Nano-Calcium Oxide from Waste Eggshell by Sol-Gel Method. *Sustainability* **2019**, *11*, 2–10.
77. Zhang, Q.; Ye, G. Dehydration Kinetics of Portland Cement Paste at High Temperature. *J Therm Anal Calorim* **2012**, *110*, 153–158, doi:10.1007/s10973-012-2303-9.
78. Zhang, Z.; Scherer, G.W. Evaluation of Drying Methods by Nitrogen Adsorption. *Cem Concr Res* **2019**, *120*, 13–26, doi:10.1016/j.cemconres.2019.02.016.
79. Shui, Z.; Xuan, D.; Chen, W.; Yu, R.; Zhang, R. Cementitious Characteristics of Hydrated Cement Paste Subjected to Various Dehydration Temperatures. *Constr Build Mater* **2009**, *23*, 531–537, doi:10.1016/J.CONBUILDMAT.2007.10.016.
80. Ermilova, E.; Kamalova, Z.; Ravil, R. Influence of Clay Mineral Composition on Properties of Blended Portland Cement with Complex Additives of Clays and Carbonates. *IOP Conf Ser Mater Sci Eng* **2020**, *890*, doi:10.1088/1757-899X/890/1/012087.

81. Moropoulou, A.; Bakolas, A.; Aggelakopoulou, E. Evaluation of Pozzolanic Activity of Natural and Artificial Pozzolans by Thermal Analysis. *Thermochim Acta* **2004**, *420*, 135–140, doi:10.1016/J.TCA.2003.11.059.
82. Castellote, M.; Alonso, C.; Andrade, C.; Turrillas, X.; Campo, J. Composition and Microstructural Changes of Cement Pastes upon Heating, as Studied by Neutron Diffraction. *Cem Concr Res* **2004**, *34*, 1633–1644, doi:10.1016/S0008-8846(03)00229-1.
83. REAL, C. Hydration Products in Two Aged Cement Pastes. *J Therm Anal Calorim* **2005**.
84. A Study of Carbonation in Non-Hydraulic Lime Mortars — the University of Bath's Research Portal Available online: https://researchportal.bath.ac.uk/en/studentTheses/a-study-of-carbonation-in-non-hydraulic-lime-mortars (accessed on 22 October 2024).
85. Ji, X.; Ji, D.; Yang, Z.; Wang, G.; Huang, X.; Ma, S.; Li, W. Study on the Phase Composition and Structure of Hardened Cement Paste during Heat Treatment. *Constr Build Mater* **2021**, *310*, 125267, doi:10.1016/J.CONBUILDMAT.2021.125267.
86. Guzhan, O.˘; Glu, Ç.˘ Revealing the Dark Side of Portlandite Clusters in Cement Paste by Circular Polarization Microscopy. *Materials 2016, Vol. 9, Page 176* **2016**, *9*, 176, doi:10.3390/MA9030176.
87. Tosun, K. Effect of SO3 Content and Fineness on the Rate of Delayed Ettringite Formation in Heat Cured Portland Cement Mortars. *Cem Concr Compos* **2006**, *28*, 761–772, doi:10.1016/J.CEMCONCOMP.2006.06.003.
88. Tran, T.T.; Kwon, H.M. Influence of Activator Na2O Concentration on Residual Strengths of Alkali-Activated Slag Mortar upon Exposure to Elevated Temperatures. *Materials 2018, Vol. 11, Page 1296* **2018**, *11*, 1296, doi:10.3390/MA11081296.
89. Thiery, M.; Villain, G.; Dangla, P.; Platret, G. Investigation of the Carbonation Front Shape on Cementitious Materials: Effects of the Chemical Kinetics. *Cem Concr Res* **2007**, *37*, 1047–1058, doi:10.1016/J.CEMCONRES.2007.04.002.
90. Alarcon-Ruiz, L.; Platret, G.; Massieu, E.; Ehrlacher, A. The Use of Thermal Analysis in Assessing the Effect of Temperature on a Cement Paste. *Cem Concr Res* **2005**, *35*, 609–613, doi:10.1016/J.CEMCONRES.2004.06.015.
91. Moropoulou, A.; Bakolas, A.; Aggelakopoulou, E. The Effects of Limestone Characteristics and Calcination Temperature to the Reactivity of the Quicklime. *Cem Concr Res* **2001**, *31*, 633–639, doi:10.1016/S0008-8846(00)00490-7.
92. Taylor, H.F.W. *Cement Chemistry*; Thomas Telford Publishing, 1997; ISBN 0-7277-3945-X.
93. Ghosh, S.N.; Rao, P.B.; Paul, A.K.; Raina, K. The Chemistry of Dicalcium Silicate Mineral. *J Mater Sci* **1979**, *14*, 1554–1566, doi:10.1007/BF00569274/METRICS.
94. Jelenić, I.; Bezjak, A.; Bujan, M. Hydration of B2O3-Stabilized A′-and β-Modifications of Dicalcium Silicate. *Cem Concr Res* **1978**, *8*, 173–180, doi:10.1016/0008-8846(78)90006-6.
95. Cruz, T.A.M. da; Henrique Geraldo, R.; Damasceno Costa, A.R.; Rândello Dantas Maciel, K.; Pereira Gonçalves, J.; Camarini, G. Microstructural and Mineralogical Compositions of Metakaolin-Lime-Recycled Gypsum Plaster Ternary Systems. *Journal of Building Engineering* **2022**, *47*, 103770, doi:10.1016/J.JOBE.2021.103770.
96. Sahmenko, G.; Sinka, M.; Namsone, E.; Korjakins, A.; Bajare, D. Sustainable Wall Solutions Using Foam Concrete and Hemp Composites. *Environmental and Climate Technologies* **2021**, *25*, 917–930, doi:10.2478/rtuect-2021-0069.

97. Collet, F.; Pretot, S. Thermal Conductivity of Hemp Concretes: Variation with Formulation, Density and Water Content. *Constr Build Mater* **2014**, *65*, 612–619, doi:10.1016/J.CONBUILDMAT.2014.05.039.
98. Gurunathan, T.; Mohanty, S.; Nayak, S.K. A Review of the Recent Developments in Biocomposites Based on Natural Fibres and Their Application Perspectives. *Compos Part A Appl Sci Manuf* **2015**, *77*, 1–25, doi:10.1016/J.COMPOSITESA.2015.06.007.
99. Ardanuy, M.; Claramunt, J.; Toledo Filho, R.D. Cellulosic Fiber Reinforced Cement-Based Composites: A Review of Recent Research. *Constr Build Mater* **2015**, *79*, 115–128, doi:10.1016/J.CONBUILDMAT.2015.01.035.
100. Collet, F.; Prétot, S.; Lanos, C. Hemp-Straw Composites: Thermal and Hygric Performances. *Energy Procedia* **2017**, *139*, 294–300, doi:10.1016/j.egypro.2017.11.211.
101. Brzyski, P.; Gładecki, M.; Rumińska, M.; Pietrak, K.; Kubiś, M.; Łapka, P. Influence of Hemp Shives Size on Hygro-Thermal and Mechanical Properties of a Hemp-Lime Composite. *Materials* **2020**, *13*, 1–17, doi:10.3390/MA13235383.
102. Abdellatef, Y.; Khan, M.A.; Khan, A.; Alam, M.I.; Kavgic, M. Mechanical, Thermal, and Moisture Buffering Properties of Novel Insulating Hemp-Lime Composite Building Materials. *Materials 2020, Vol. 13, Page 5000* **2020**, *13*, 5000, doi:10.3390/MA13215000.
103. Bumanis, G.; Irbe, I.; Sinka, M.; Bajare, D. Biodeterioration of Sustainable Hemp Shive Biocomposite Based on Gypsum and Phosphogypsum. *Journal of Natural Fibers* **2022**, *19*, 10550–10563, doi:10.1080/15440478.2021.1997871.
104. Arnaud, L.; Gourlay, E. Experimental Study of Parameters Influencing Mechanical Properties of Hemp Concretes. *Constr Build Mater* **2012**, *28*, 50–56, doi:10.1016/J.CONBUILDMAT.2011.07.052.

Pauls Pāvils Ārgalis was born in 1996 in Riga. He obtained a Bachelor of Engineering in Materials Science in 2018 and a Master of Engineering in Materials Science in 2021 from Riga Technical University. He has been working at Riga Technical University since 2020, initially as a scientific assistant in the Institute of General Chemical Engineering at the Faculty of Materials Science and Applied Chemistry, and currently as a researcher in the Institute of Sustainable Building Materials and Engineering Systems at the Faculty of Civil and Mechanical Engineering. He has worked as a project assistant in "KV Consulting" in the fields of GHG emission calculations and optimisation of biomethane production facilities. His scientific interests are related to the reactivation of cement binder, sustainable building material production and circular manufacturing.